Quantitative characterization of the sedimentary architecture of Gilbert-type deltas

Soma Budai, Luca Colombera, Nigel P. Mountney

Fluvial, Eolian & Shallow-Marine Research Group, School of Earth & Environment, University of Leeds, Leeds, LS2 9JT, UK

Corresponding author: Soma Budai, email: s.budai@leeds.ac.uk, address: School of Earth & Environment, University of Leeds, Leeds, LS2 9JT, UK

Abstract

Steep-fronted Gilbert-type deltas are common features of tectonically active settings, as well as of physiographic settings where accommodation is dictated by landforms with steeply inclined margins, such as incised valleys, fjords, and proglacial lakes. Existing facies models for Gilbert-type deltas are largely qualitative; this study presents a quantitative analysis of the variability in facies architectures of such deltas. A database approach is used to characterize the preserved sedimentary architecture of 62 Gilbert-type deltas of Cretaceous to Holocene ages developed in various basin settings worldwide. Data on 706 architectural elements and 12,872 facies units are used to develop quantitative facies models that describe the variability in architecture and facies of Gilbert-type deltas at multiple scales of observation, and to account for the possible controls exerted by allogenic and autogenic factors.

The analysed data reveal high variability in the geometry and facies of Gilbert-type deltas. The thickness of the examined deltas varies from 2 to 650 m, yet positive scaling between delta thickness and length is consistently recognized across the studied examples, which is interpreted in terms of relationships between accommodation, sediment supply and delta lifespan. Based on their facies character, the deltas are classified into gravel- and sand-dominated types, with contrasting facies organizations of topset, foreset and bottomset elements, and by different relationships between facies and dimensions; yet, both types exhibit significant spatial variability in the distribution of sediments linked to debris flows or turbidity currents, and in vertical stratal trends. Changes in allogenic (e.g., changes in base-level or, rate of sediment influx) and autogenic mechanisms (e.g., channel avulsion) are inferred as causes for significant differences in facies organization, both across distinct deltas and within individual deltaic edifices.

The study highlights the marked variety of architectural and sedimentological (e.g., grain size, depositional processes) properties of Gilbert-type deltas. Findings allow the relation of outcrop observations to a general template and the quantitative determination of potential analogues with which to assist the prediction of the dimensions and facies of deltaic sedimentary bodies in the subsurface. Information on facies relationships and basinward variability of Gilbert-type deltas is valuable for the recognition and correlation of deltaic bodies in the subsurface.

Keywords: Gilbert-type deltas, facies models, sedimentary architecture, quantitative sedimentology, allogenic factors.

1 Introduction

Gilbert-type deltas are steep-fronted sediment bodies that can develop where a fluvial feeder system debouches into a relatively deep basin characterized by an abrupt topographic change at its margin (Gilbert, 1885; Postma, 1990). Gilbert-type deltas form in a variety of tectonically active settings, including extensional, compressional, and transtensional basins. They are also common in high-relief physiographic settings where accommodation is not primarily created by tectonics, such as incised valleys, fjords, or proglacial lakes; they can even form in lakes inside volcanic craters (Nemec et al., 1999; Németh et al., 2001; Gutsell et al., 2004; Kostic et al., 2005; Eilertsen et al., 2011; Gobo et al., 2014a; Leszczyński and Nemec, 2015; Winsemann et al., 2018). These deltas form important nodes in sediment-delivery pathways linking continental hinterlands to subaqueous lacustrine (Bowman, 1990; Bestland 1991; Lee and Chough, 1999; Ilgar and Nemec, 2005; Sztanó et al., 2010) and marine depocentres (Colella, 1988; Mortimer et al., 2004, 2005; García-García et al., 2016a; Breda et al., 2009; Ciampalini and Firpo, 2015; Rees et al., 2018).

Allogenic forcing by climate, tectonics and eustasy acts to control factors that influence delta evolution, such as basin depth and morphology, catchment-area bedrock and physiography, and variations in base level, water discharge and sediment supply. All these factors can influence the geometry of the prograding deltas and their architectural elements. They can also influence the predominance of different depositional processes, themselves determining distributions of grainsize and sedimentary structures, and thereby lithofacies (Colella, 1988; Postma, 1995; Gupta et al., 1999; Breda et al., 2009; Gobo et al., 2014a, 2014b, 2015; Martini et al., 2017; Winsemann et al., 2018, 2021). The role of autogenic mechanisms in shaping the evolution and stratigraphic record of these deltas is also recognized. For example, the width of feeder systems controls vertical grainsize trends in deltaic foresets (Kleinhans, 2005), whereas delta-lobe switching is driven by mechanisms of channel avulsions (Longhitano, 2008). However, in spite of current understanding, facies models for Gilbert-type deltas and their preserved successions are largely qualitative; a systematic and quantitative analysis of the variability in facies architectures of Gilbert-type deltaic successions has yet to be produced.

The aim of this study is to develop a novel suite of quantitative facies models for Gilbert-type deltas based on the integration of sedimentological data from many known examples. Specific objectives of this work are as follows: (i) to characterize quantitatively the variability seen in the architecture and facies of Gilbert-type deltas, at multiple scales of observation; and (ii) to relate observed differences in architecture and facies organization to the possible controls exerted by allogenic and autogenic factors. This study uses a database-driven approach to the synthesis of sedimentological datasets.

2 Background

Gilbert-type deltas were first described by Grove Karl Gilbert (1885) from the Pleistocene Lake Bonneville (Utah, USA). They are steep-fronted sedimentary bodies, characterized by 20°-35° delta-front dip, and form where alluvial feeder systems debouche into basins characterized by steep gradients. Deltas of this type can develop over a range of water depths, they can form in relatively shallow water, as long as the basin margins on which they sit is sufficiently steep and delta-plain processes are dominated by mass flows and partly unconfined stream flows. This situation contrasts

with that of more gently sloping basin margins and of settings with dominantly channelized flows, which instead tend to favour the formation of mouth-bar deltas (Dunne and Hempton, 1984; Postma 1990). Gilbert-type deltas are characterized by a unique tripartite internal architecture, consisting of topsets transitioning to steeply inclined (20°-35°) foresets representing the subaqueous delta slope, themselves passing downdip into subhorizontal to gently inclined (up to 10°) bottomsets (Gilbert, 1885; Barrell, 1912; Postma, 1990; Smith and Jol, 1997) (Fig. 1A,D). This distinctive sedimentary architecture has been reported from many outcrop-based studies, and is also documented by geophysical datasets, such as ground-penetrating radar (GPR) surveys (e.g., Smith and Jol, 1997; Gutsell et al., 2004; Kostic et al., 2005; Eilertsen et al., 2011) or high-resolution seismic datasets (e.g. Winsemann et al. 2018). The gradual, tangential transition from foreset to bottomset defines a physiographic element that is commonly referred to as a toeset (Breda et al., 2007, 2009; Ghinassi, 2007; Gobo et al., 2014b; Rubi et al., 2018). In some cases, bottomsets may be lacking altogether, for example during the early stages of delta evolution (Colella, 1988; Mortimer et al., 2004, 2005) (Fig 1), or through progradation in sub-basins confined by topographic highs (Zelilidis and Kontopoulos, 1996). The deltaic foresets pass updip into fluvial or alluvial deposits (Colella, 1988; Ilgar and Nemec, 2005) arranged into topset geometries. Deltas with alluvial-fan feeder systems are commonly referred to as Gilbert-type fan deltas (Colella et al., 1987; Nemec and Steel, 1988; Postma, 1990; Dorsey et al., 1995; Hwang and Chough, 2000; Rees et al., 2018). The transition between the delta slope and the updip delta plain can be erosional, or either sharp or gradual when associated with sigmoidal geometries and preservation of a delta brink point (Rohais et al., 2008; Gobo et al., 2014a, 2015) (Fig. 1C,D). The type of foreset-topset transition depends on hydrodynamic conditions and associated sub-environments (e.g., fluvial channels, mouth bars), and on short-term base-level changes (Gawthorpe and Colella, 1990; Massari and Parea, 1990; Longhitano, 2008; Gobo et al., 2015; Winsemann et al., 2018). Sigmoidal geometries are associated with relative base-level rise, and therefore with an increased preservation of the sediments deposited at the topset-to-foreset transition, a physiographic element referred to as 'delta front' in some studies (Colella, 1988; Soria et al., 2003; García-García et al., 2006a; Longhitano, 2008; Gobo et al., 2014a, 2015).

The three main elements of Gilbert-type deltas are themselves composed of smaller-scale sedimentary bodies associated with different sub-environments and depositional processes depending on the depositional setting (e.g., lacustrine, glacial or volcanic). The diversity in sedimentary architecture can be especially noteworthy on the topset and at topset-to-foreset (delta-front) transition, where different types of architectural elements are formed in sub-environments of alluvial systems, and due to the interaction between fluvial and basinal processes at the river mouth. On the delta plain, streamflow processes typically produce laterally shifting braided channels, in which barforms of different types can be deposited (Kostic et al., 2005; Rohais et al., 2008; Gobo et al., 2015; Ilgar, 2015; Leszczyński and Nemec, 2015), and whose mobility can lead to the limited preservation of finer-grained overbank deposits (Dart et al., 1994; Longhitano, 2008). In addition, deposits of subaerial debris flows are also seen to constitute portions of topsets, especially in association with alluvial-fan feeder systems (Ghinassi, 2007; Ilgar and Nemec, 2005). Wave action at the delta front can be manifested in the reworking of alluvial sediments and in the formation of beach deposits (Massari and Parea, 1990; Lønne and Nemec, 2004; Longhitano, 2008; Gobo et al., 2014a; García-García et al., 2016b; Rees et al., 2018).

Delta slopes are dominated by a wide range of types of subaqueous sediment gravity flows (Nemec, 1990; Chough and Hwang, 1997; Sohn et al., 1997; Falk and Dorsey, 1998; Ferentinos et al., 1988; McConnico and Bassett, 2007; Gobo et al., 2014). These include debris flows, debris falls, turbidity currents of both high and low density (Lowe, 1982), and slumping (Postma, 1984; Nemec et al., 1999; Leszczyński and Nemec, 2015). Debris flows, debris falls and surge-like turbidity currents are commonly generated by delta-front collapses, which can be triggered by the following: (i) oversteepening of the slope due to excess sediment accumulation (Nemec et al., 1999; Gobo et al., 2015); (ii) minor base-level fluctuations (Postma and Roep, 1985); (iii) storm-wave erosion in response to flood-induced hyperpycnal flows (Gobo et al., 2015); or (iv) seismic shaking (Ferentinos et al., 1988; Gobo et al., 2014b). Mud tends to be winnowed by wave reworking and transported away from the shoreline by buoyant hypopycnal plumes. As such, debris flows occurring down the slope are commonly cohesionless; hence foreset deposits tend to be devoid of mud even in cases where the fluvial feeder system is characterized by a relatively high mud content (Chough et al., 1990; Nemec, 1990, 1995; Sohn et al., 1997; Gobo et al., 2014b). Sustained turbidity currents can also take place on delta slopes, in relation to pulsating hyperpycnal flows during river floods (Gobo et al., 2014a).

The morphology of the delta slope can be segmented by ridges, chutes, debris-flow mounds, slump blocks and slide scars. Chutes cut by turbidity currents (Nemec, 1990; Prior and Bornhold, 1990) can promote the development of confined turbulent flows, which may become supercritical and undertake a hydraulic jump while encountering obstacles on the delta slope and at the delta toe (e.g., debris-flow mounds; Massari, 1996; Nemec et al., 1999; Gobo et al., 2014b). Deposition from supercritical flows that underwent hydraulic jumps is manifested in lobate sedimentary bodies (Nemec et al., 1990, 1999; Breda et al., 2007) forming at chute outlets due to flow deceleration and expansion (Fig. 1A), and in upslope-dipping solitary backsets, which typically fill spoon-shaped scours (Massari and Parea, 1990; Massari, 1996; Ilgar and Nemec, 2005; Breda et al., 2007, 2009; Leszczyński and Nemec, 2015; Massari, 2017). In some cases, backsets are interpreted as the preserved structures of chute-and-pool bedforms (Lang and Winsemann, 2013; Lang et al. 2017). Supercritical flows are also capable of forming antidunes and cyclic steps on the subaqueous part of a delta (Lang et al., 2017, 2021; Rubi et al., 2018; Winsemann 2018, 2021; Postma et al. 2021). These structures can be especially common, even predominant, in the deposits of Gilbert-type delta foresets in glaciogenic depositional settings, where high-energy, rapid meltwater flows favour the formation of supercritical density flows (Lang et al., 2017, 2021; Winsemann et al., 2018). Typically, delta bottomsets are principally made of turbidites generated either by flood-induced hyperpycnal flows that bypassed the delta slope, or by debris-flow transformation due to dilution by water entrainment and/or sedimentation of their coarser load on delta slopes or toes (Dorsey et al., 1995; Sohn et al., 1997; Falk and Dorsey, 1998; Ilgar and Nemec, 2005; Gobo et al., 2014b); this type of flow transformation can occur over short distances (10-20 m) (Falk and Dorsey, 1998). At the delta toe, high-density turbidity currents tend to drop their coarser load due to flow expansion and deceleration, and as such only their finer-grained load may reach the bottomset (Ilgar and Nemec, 2005). These processes tend to deposit finer bottomsets compared to the overlying foreset. However, after their incision by bypassing currents, delta-slope chutes that extend beyond the foreset can facilitate the transport of sediment from the delta brink or chute wall to the delta toe, which can result in the preservation of conglomeratic debris-flow-dominated channel fills (Nemec, 1990;

Gobo et al., 2014b). Both the importance of suspension settling and the proportion of mud tend to increase basinward (Massari and Parea, 1990; Breda et al., 2007).
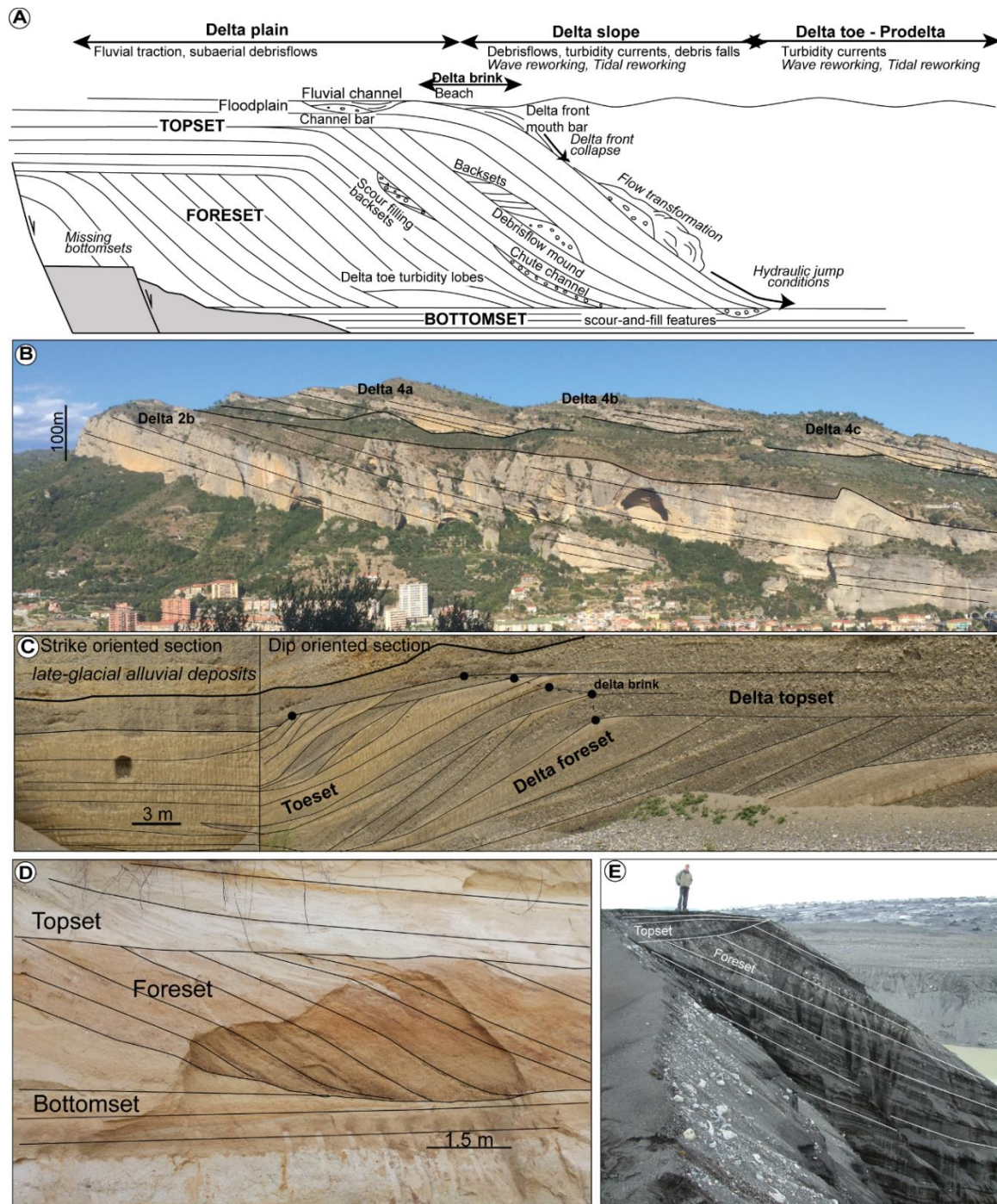

Figure 1 Examples of Gilbert-type deltas and nomenclature used in the description of their morphology and deposits. (A) Schematic cross section of a Gilbert-type delta showing its tripartite internal architecture, smaller-scale architectural elements and other features. No scale intended. (Compiled after Colella, 1988; Falk and Dorsey, 1998; Longhitano, 2008; Gobo et al., 2014b). (B) Stacked Gilbert-type deltas in the Pliocene of Ventimiglia, Italy; for detailed interpretation see Breda et al. (2007). (C) Perspective view over dip- and strike-oriented sections of a Pleistocene Gilbert-type delta from the Aar Valley, Switzerland (photo courtesy of Ilaria Menga). (D) Small-scale sandy Gilbert-type delta in the Miocene of the Vienna Basin, Austria. (E) Large scale, gravel-dominated topsets and foresets representing the deposits of a Gilbert-type fan-delta. Recent, Skeiðarársandur, southern Iceland.

3 Data and methods

A database approach has been used to synthesize sedimentological data from the preserved successions of 62 Gilbert-type deltas, related to 14 case studies (Table 1) and originally presented in 18 published sources. These case studies are referred to throughout the article using the acronyms reported in Table 1. The data are stored in the Shallow-Marine Architecture Knowledge Store (SMAKS), a relational database that stores qualitative and quantitative data on shallow-water and paralic sedimentary units of different types and scales (e.g., facies, architectural elements), and on the depositional context in which the successions were accumulated (Colombera et al., 2016). The datasets considered for this synthesis are based on field studies of outcropping successions. Only case studies that contain data on multiple architectural elements and facies were selected; studies that specifically focus on individual elements were excluded.

In SMAKS, architectural elements are sedimentary bodies with characteristic facies associations and architectural properties, usually interpretable in terms of a particular sub-environment of deposition. Architectural elements can develop over a range of hierarchies, recorded in the database through parent-child relationships (e.g., delta-top element containing alluvial channel fills; Fig. 3). Architectural elements can contain several facies units, i.e., elementary lithological units with sub-bed scale resolution, whose subdivision reflects changes in sediment texture, structure, palaeoflow direction, and/or the presence of intervening surfaces marking erosion or breaks in sedimentation (Fig. 3). Architectural elements, and associated facies units, can be contained in sequence stratigraphic units (e.g., systems tracts, parasequences) and are bounded by surfaces of different types, which may also have sequence-stratigraphic significance (Fig. 3).

Quantitative data on the geometry of architectural elements, facies and sequence stratigraphic units were extracted from figures presenting outcrop panels and sedimentary logs, using image-analysis software (ImageJ; Schneider, 2012), or directly from the text. Spatial relationships between different units of the same rank (architectural elements and facies) were also recorded, in the form of transitions in the vertical, downdip and along-strike directions. Architectural elements were variably classified according to sub-environment of deposition, architectural types, process dominance and shape. Facies units were classified on several attributes, including grainsize (overall and modal grainsize of sand fraction), sedimentary structure, grading and interpreted depositional processes.

Collectively, 706 architectural elements and 12,872 facies units related to 62 Gilbert-type deltas were considered. The relational nature of the database enables filtering the data on any combination of attributes of sedimentary units and depositional systems (Colombera et al., 2016).

The thickness of the elements was measured from figures in the original data sources, capturing values of maximum thickness from architectural panels; thickness data were also recorded from the text where 'maximum' values were reported. The vertical dimensions of elements that were only represented on sedimentary graphic logs were reported as 'apparent', and only considered if underlying and overlying sedimentary bodies were recorded. Element thickness is classified as 'partial' if either of the element boundaries are not observed, or 'unlimited' if both of the element boundaries are not observed (Geehan and Underwood, 1993) (Fig. 3). Element length was measured from

the updip termination (e.g., delta nucleation point) to the basinward termination of the element (e.g., base of the delta slope). Similarly to thickness values, element lengths are classified as 'partial', 'unlimited' or 'apparent' (Fig. 3). In the statistical analyses of element geometry (e.g., thickness vs. length), only entities with apparent and maximum thickness were used. Similarly, when examining vertical facies trends and relating facies data to element thickness, only elements whose vertical extent could be seen in full were considered (i.e., elements whose underlying and overlying elements were observed). When extracting facies proportions, all elements were used regardless of their thickness type. Proportions of facies characterized by a specific attribute (e.g., grainsize, depositional process) were calculated as fractions of cumulative thickness.

Statistical analyses were performed to determine relationships between different quantitative characteristics of the studied palaeo-deltas. Pearson and Spearman correlation coefficients were calculated (respectively indicated with R and r, hereafter) for pairs of continuous variables, with their statistical significance expressed as P-values (P and p, for Pearson and Spearman coefficients respectively, hereafter). The primary data presented in this paper are included as Supplementary material.

Figure 2 Geographic location of the considered Gilbert-type deltaic successions.

Figure 3 Idealized fictional example of how geological entities of Gilbert-type deltaic successions are stored in the SMAKS database (Colombera et al., 2016). These include architectural elements and their

Case study name	Case study code	Location	Nr of deltas	Age	Basin	Basin type	Tectonic setting	Environmental /Depositional setting	Reference
Holocene Hiorthfjellet fan delta	HFJ	Spitsbergen	1	Holocene				Marine, fjord	Lönne and Nemec (2004)
Akrata incised valley	AKR	Greece	1	Pleistocene	Gulf of Corinth Basin	Continental rift	Extensional	Marine, incised valley	Gobo et al. (2014a)
Kregnes moraine	KRE	Norway	1	Pleistocene				Marine, fjord	Nemec et al. (1999)
Middle Group of Corinth Rift	MGCR	Greece	2	Pleistocene	Gulf of Corinth Basin	Continental rift	Extensional	Marine	Gobo et al. (2014b and 2015); Rubi et al. (2018)
Pliocene of Potenza Basin	POT	Italy	5	Pliocene	Potenza Basin	Piggy-back basin	Convergent	Marine	Longhitano (2008)
Pliocene of Loreto Basin	LOR	Mexico	14	Pliocene	Loreto Basin		Trans-tensional	Marine	Mortimer (2004); Mortimer et al. (2005)
Pliocene of Val d'Orcia Basin	VdO	Italy	7	Pliocene	Val d'Orcia Basin		Extensional	Marine	Ghinassi (2007)
Pliocene of Ventimiglia	VEN	Italy	12	Pliocene				Marine, incised-valley	Breda et al. (2007 and 2009)
Gelincik Formation	GEL	Turkey	2	Miocene	Central Pontide Miocene Foredeep	Retroarc foreland basin	Convergent	Marine, incised-valley	Ilgar (2015)
Miocene of Polish Carpathian Foredeep	PCF	Poland	1	Miocene	Polish Carpathian Foredeep	Peripheral foreland basin	Convergent	Marine	Leszczynski and Nemec (2017)
Miocene of Western Carpathian Foredeep	WCF	Czech Rep.	2	Miocene	Western Carpathian Foredeep	Peripheral foreland basin	Convergent	Marine	Nehyba (2018)
Yenimahalle Formation	YEN	Turkey	6	Miocene	Ermenek Basin	Backarc basin	Strike-slip	Lacustrine	Ilgar and Nemec (2005)
Roda Formation	ROD	Spain	7	Eocene	Tremp-Graus Basin	Piggy-back basin	Convergent	Marine	Leren et al. (2010)
Upper Cretaceous of Jinan Basin	JIN	South Korea	1	Cretaceous	Jinan Basin	Trans-tensional	Strike-slip	Lacustrine	Lee and Chough (1999)

Table 1 Account of SMAKS (Shallow Marine Architecture Knowledge Store; Colombera et al., 2016) case studies considered in this work.

4 Results

4.1 Delta dimensions

The Gilbert-type deltas discussed in this study vary in thickness from ca. 2 m to 650 m (Fig. 4). The majority of the examined deltaic bodies (75%) are less than 50 m thick, and 40% of the examples are less than 10 m thick. Their downdip length varies between 114 m and 6000 m. Thickness-to-length ratios range from 1:10 to 1:80. Most of the deltaic sedimentary bodies whose geometry can be characterized (8 out of 15 deltas), are 10 to 20 times longer than thicker. Considering only cases where the whole length of the delta body was captured (N=15) a positive correlation can be seen between delta thickness and length (R=0.70, P=0.004, r=0.85 p<0.001).

Case studies containing multiple deltas (9 out of 14 case studies) demonstrate high variability in delta dimensions (Fig. 4D), whereby the thickness of the smallest deltas can be as small as 20% of that of the largest one in the same setting. This was observed in the case of small (<10 m; e.g., YEN, GEL; see Table 1 for abbreviations) and large deltas (>30 m; e.g., VEN, WCF) alike. Similarly, delta lengths can vary significantly within case studies, by factors of ca. 6 (e.g., LOR) to at least 12 (e.g., VEN).
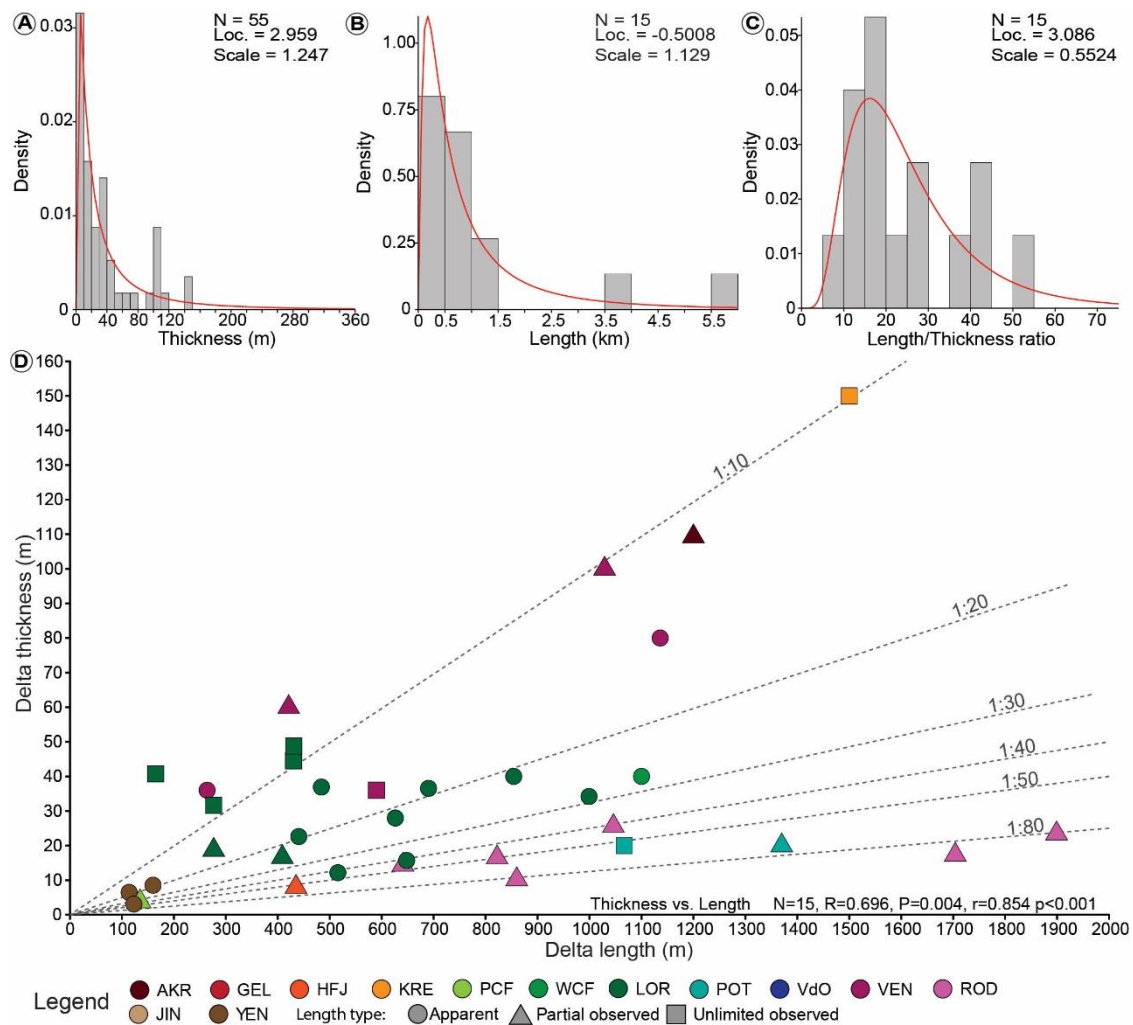
Figure 4 Histograms showing distributions in thickness (A), length (B) and length-to-thickness ratio (C) of the studied deltaic bodies, each with a fitted log-normal distribution. In B and C, only data on apparent or maximum length were used. (D) Scatter plot of the thickness versus length of studied Gilbert-type
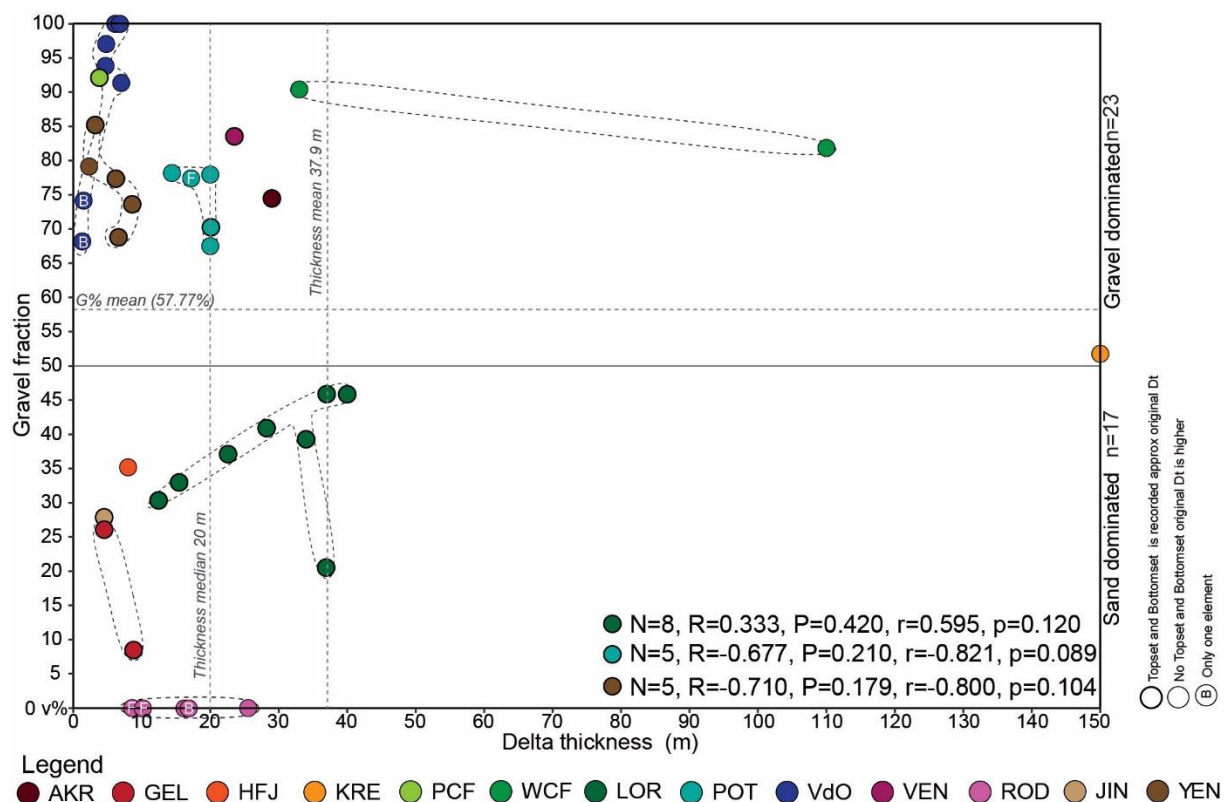
deltaic bodies (N denotes the sample number, R: Pearson's R, r: Spearman's rho). Case study codes can be found in Table 1.

4.2 Delta facies

The gravel fraction of the examined deltas (encompassing all types of deltaic elements) is highly variable: the studied deltas range from being made entirely of sandy facies units to containing almost exclusively gravels (Fig. 5). In 25 out of 42 deltas with quantifiable facies data, the proportion of gravelly facies exceeds 50%; these deltas are termed here as gravel-dominated deltas, in contrast with sand-dominated deltas containing in excess of 50% of sandy facies. In each case study, all deltas belong exclusively to either of the groups; however, variations in the proportion of gravelly facies can be as high as 25% (Fig. 5).

No noticeable trend is observed between the fraction of gravelly facies and the thickness of the deltas. Individual case studies, such as the Yenimahalle Fm. and the Potenza Basin fill (Table 1), show negative correlation between these two variables, but these are not statistically significant (N=5, R=-0.710, P=0.179, r=-0.800, p=0.104 and N=5, R=-0.677, P=0.210, r=-0.821, p=0.089 respectively). A positive relationship can be seen in the examples from the Loreto Basin fill (N=8, R=0.33, P=0.420, r=0.595, p=0.120) (Fig. 5).

Figure 5 Scatter plot of the thickness versus gravel fraction of studied Gilbert-type deltas (N denotes the sample number, R: Pearson's R, r: Spearman's rho). Case study codes can be found in Table 1.

4.3 Delta elements

Although the tripartite internal architecture that is diagnostic of Gilbert-type deltas was recognized in all of the studied examples, only half of the 44 examined vertical sedimentary sections that capture the entire vertical profile of the deltas (i.e., from base to top) record complete successions of bottomset, foreset and topset elements (Fig.

6). Delta-top deposits were only present above the delta slope in 65% (n=53) of the examined sedimentary sections. In 23% (n=52) of the sections, foreset elements were not underlain by a bottomset element (Fig. 6). In most cases, topset absence was caused by erosion due to base-level fall; more rarely, the lack of a topset reflects how sedimentary logs were measured basinward of the point of maximum delta brink progradation (e.g., LOR, VdO). The absence of delta-toe deposits depends on the position of the sedimentary logs, as bottomsets may not have developed in proximity of the delta nucleation point but might instead be present in sections located farther basinward, as depicted in Fig. 1 (Colella et al., 1987; Leszczyński and Nemec, 2015; Mortimer et al., 2004, 2005).
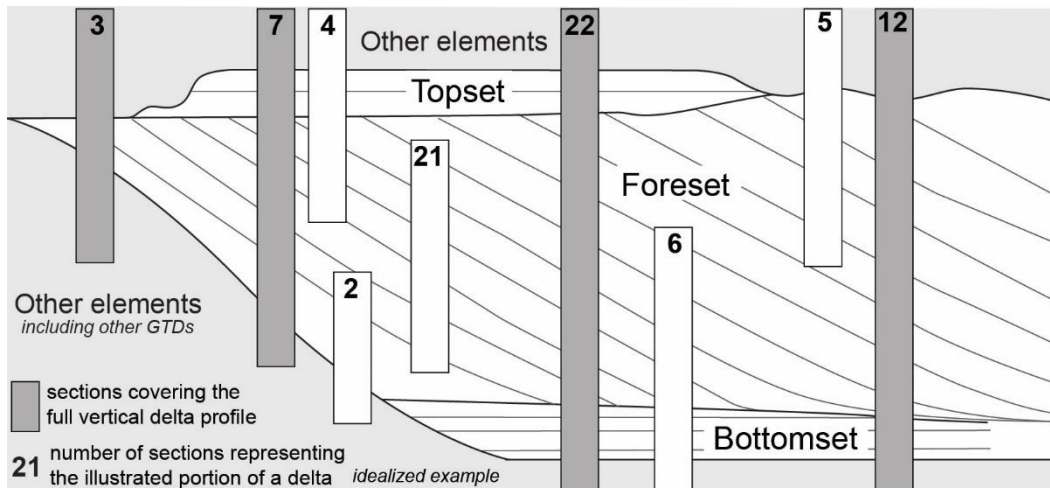
Figure 6 Schematic representation of the stratigraphic coverage of the examined sedimentary logs, illustrating the frequency with which they span the elements of Gilbert-type deltas. The numbers inside the columns represent the number of occurrence of the specific element sequence illustrated on the section. Sections intersecting the whole preserved deltaic body (i.e.including base and top) are coloured in grey. No scale intended.

4.3.1 Element proportions

Proportions of the three characteristic elements of Gilbert-type deltas, based on cumulative thickness, vary between different deltaic successions, ranging from examples where the three elements are present in approximately equal fractions (e.g., POT), to examples where foreset packages represent 98% of the vertical profile of the delta (e.g., GEL, VdO, LOR). In cases where specific deltaic bodies were characterized over multiple sections or 2D panels, the vertical dimensions of deltaic successions and their constitutive elements were measured where the delta is thickest; only successions in which the full vertical profile of the delta was captured were included in the analysis (Fig. 6). As delta topsets are commonly missing (Fig. 6), whereas bottomsets are present in all examined cases, the studied examples have been grouped based on the thickness of foreset elements relative to the cumulative thickness of foresets and bottomsets. By binning this thickness ratio, four groups are defined, each of which covers a range of thickness ratio equal to 0.1, and which collectively cover a range from 0.57 to 0.97 (Fig. 7). The studied deltas are uniformly distributed across these groups, each of which is further characterized in terms of average relative thickness of topset, foreset and bottomset elements (Fig. 7). Compared to bottomsets, topset proportions are generally lower and less variable (Fig. 7). The examined successions in which delta toesets were distinguished were only

11

observed in sections that do not encompass the full profile of the deltaic body; hence, these examples were not used in this analysis.
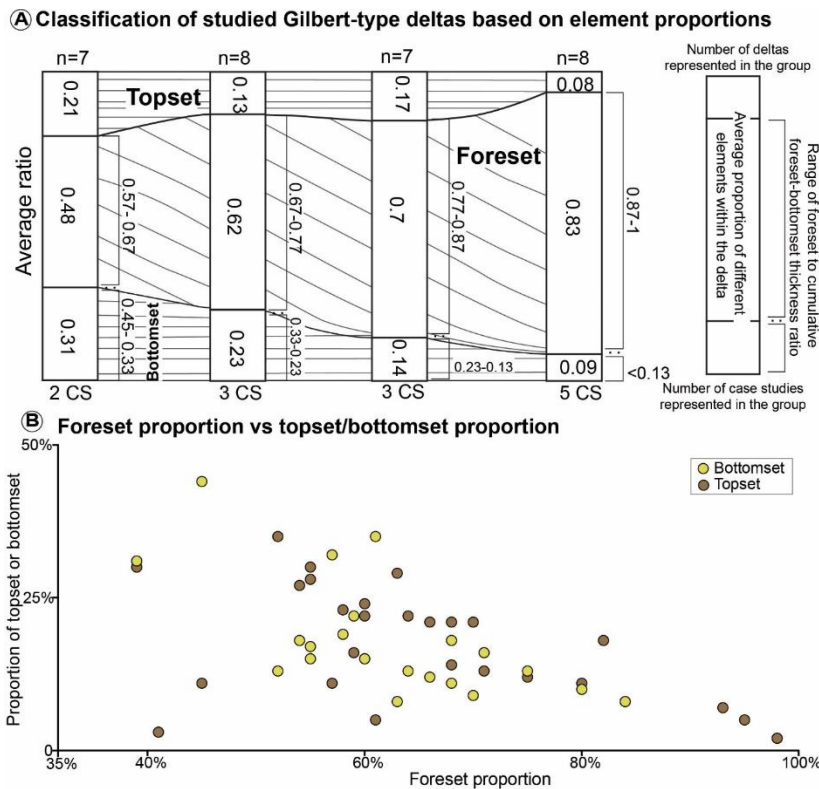

Figure 7 (A) Proportions of architectural elements of the studied deltas, grouped in four categories based on binning of the ratio between foreset thickness and cumulative foreset-bottomset thickness. CS = case study. (B) Scatterplot showing the proportion of topset and bottomset deposits relative to the proportion of foreset deposits in the studied delta edifices.

4.3.2 Element facies

4.3.2.1 Grainsize

The fraction of gravelly facies in distinct deltaic elements varies markedly between gravel- and sand-dominated deltas, as is expected. However, in 89% of the cases a gradual coarsening trend is observed from the delta toe to the delta top (Fig. 8). Gravel-dominated deltas are composed of coarse topset and foreset (mean gravel proportions above 75%), whereas their bottomset deposits vary more significantly in terms of grainsize, from being made exclusively of sandy facies to being fully gravelly, with an average gravel percentage of 33% (Fig. 8).

In contrast, in the slopes and bottomsets of sand-dominated deltas, gravelly facies are generally subordinate (mean proportions of 22% and 6%, respectively). In these deltas, foreset elements show a higher variability in grainsize compared to gravel-dominated ones, whereas bottomsets never exhibit more than 25% of gravelly facies. Delta-top deposits of sandy deltas show a wide range of modal grainsizes, albeit containing a markedly reduced fraction of gravelly facies in comparison to their gravel-dominated counterparts (mean proportions: 60% vs. 90%); however, they remain gravel-prone in the majority of cases (Fig. 8). For sand-dominated deltas, the largest difference in the content of gravelly facies is seen between topset and bottomset deposits. The proportion of gravels also varies widely across distinct element types of the same depositional systems (Fig. 9), with a difference of up to 50% (e.g., LOR foresets, YEN

12

bottomsets) between maximum and minimum values. This high grainsize variability is not restricted to a specific type of deltaic element.

In nearly every delta, coarsening-upward trends are well-expressed, whereby foreset elements tend to contain less gravelly facies than their associated topsets (28 out of 31 deltas) but more gravels relative to the underlying bottomsets (23 out of 24 deltas) (Fig. 9). For gravel-dominated deltas this coarsening-upward trend is usually characterized by a prominent decrease in gravel content between foresets and bottomsets, occasionally resulting in sandy bottomsets that are sharply overlain by gravel-rich delta slopes (MPCF, PVOB); however, in certain depositional systems (e.g., in the Potenza basin) a more gradual grainsize trend is observed.

Comparing the fraction of gravelly facies in genetically related elements (Fig. 9), a strong positive correlation is seen between the gravel proportions of topsets and underlying foreset elements in gravel-dominated deltas (N=10, R=0.860, P<0.001, r=0.900, p<0.001), while a moderate negative relationship is instead observed for sand-dominated deltas (N=11, R=-0.562, P=0.072, r=0.607, p=0.048). A weak negative correlation exists between fractions of gravelly facies in the foresets and bottomsets of coarse-grained deltas (N=15, R=-0.257, P=0.356, r=-0.363 p=0.183), whereas no correlation is observed between the same variables in sand-dominated deltas (N=9, R=-0.127, P=0.746, r=-0.205 p=0.596).
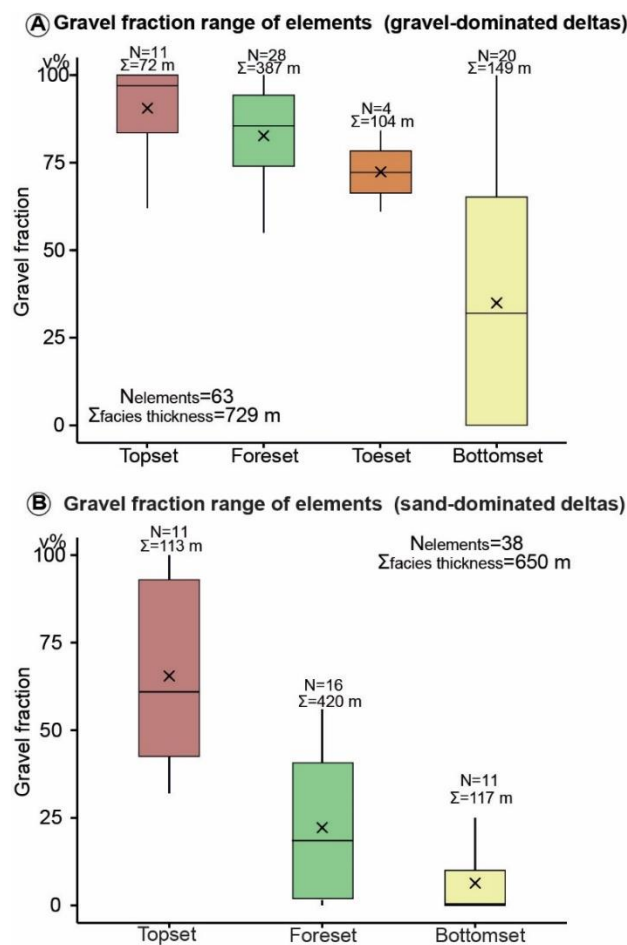

Figure 8 Boxplots showing distributions of gravel fractions in architectural elements of gravel-dominated (A) and sand-dominated (B) Gilbert-type deltas. Delta toesets were only differentiated in three case studies, containing gravel-dominated deltas, and the majority of the toeset data is from the MGCR dataset (96 m out of 104 m of total logged thickness).

The examined deltaic successions are variably made of gravel, sand and gravelly sand facies, and are in most cases (11 out of 14 case studies) devoid of any significant amount of mud (Fig. 10). Gravelly sands are more common than purely sandy facies in 40% of the foresets, and are subordinate in nearly every topset and bottomset. No correlation is observed between the contents of gravels and pebbly sands of individual elements. In cases where they are present, muddy sediments only constitute 1% to 2% of topset and foreset deposits, but can make up a larger fraction of the bottomsets, especially in association with deltas characterized by thicker foresets and higher slopes (MGCR and WCF).
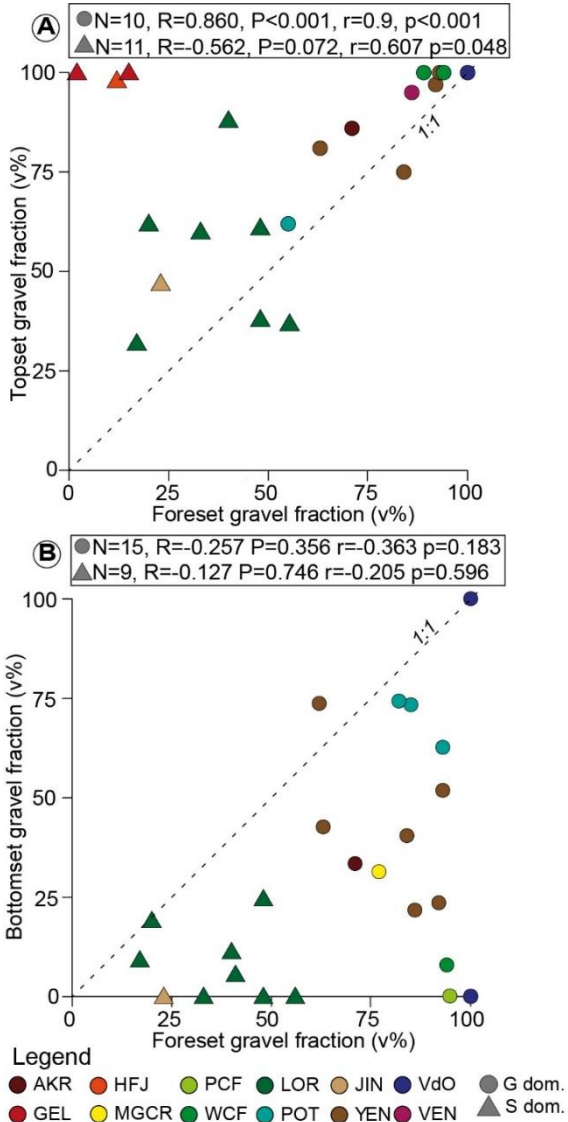
Figure 9 Scatterplots of gravel fractions of foreset versus overlying topset (A), and gravel fractions of foreset versus underlying bottomset (B). N denotes the sample number, R: Pearson's R, r: Spearman's rho. Case study codes can be found in Table 1.
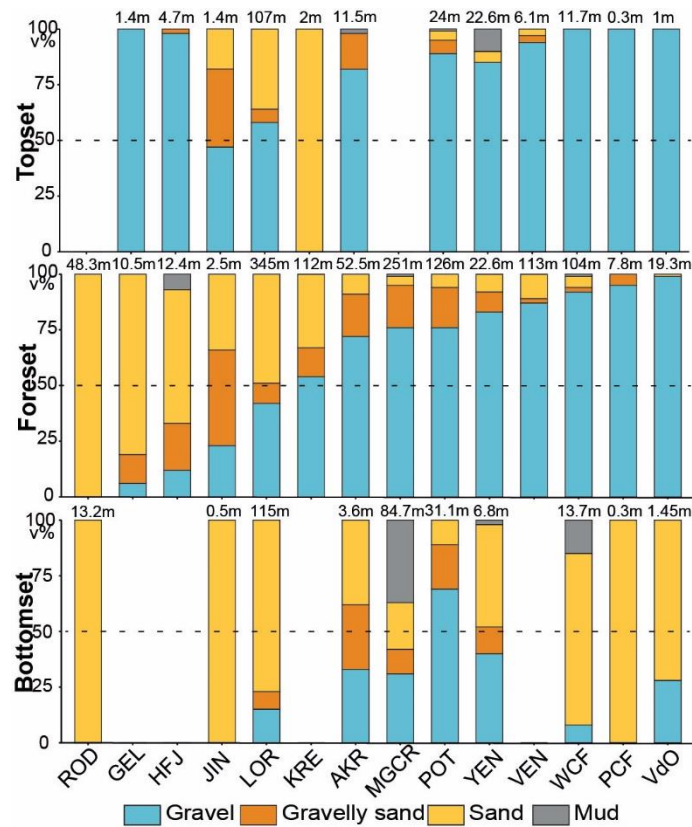
Figure 10 Stacked bar charts showing the proportions of different grainsize facies in distinct elements of the studied Gilbert-type deltas. Cumulative facies thicknesses on which the data are based are reported above each bar. Case study codes can be found in Table 1.

4.3.2.2 Element grainsize vs. dimensions

For both gravel- and sand-dominated deltas, an inverse moderate relationship is seen between the fraction of gravel facies in foresets and the foreset thickness (Fig. 11). The delta slopes of coarse deltas tend to contain proportionally higher amount of sand where foresets are thicker, i.e., where the slopes can be inferred to have been higher (N=19, R=-0.344, P=0.149, r=-0.491, p=0.033); gravel fraction values above 85% are restricted to foresets thinner than 5 m. In contrast, the foresets of sand-dominated deltas tend to be coarser where thicker (N=15, R=0.511, P=0.052, r=0.515, p=0.050).

No correlation is seen between the proportion of gravelly facies and the thickness of either topsets or bottomsets (Fig. 11), although a positive correlation between bottomset thickness and gravel content is seen specifically in examples from the Loreto Basin (N=8, R=0.738, P=0.037, r=0.741, p=0.036) (Fig. 11). As the sediment distribution to the delta toe can be affected by the length and height of the delta slope, the relationship between foreset thickness and bottomset facies was also examined. No overall trend could be observed, although a strong negative correlation between foreset thickness and bottomset gravel content is seen in examples from the Potenza Basin (N=4, R=-0.988, P=0.012, r=0.800, p=0.200).
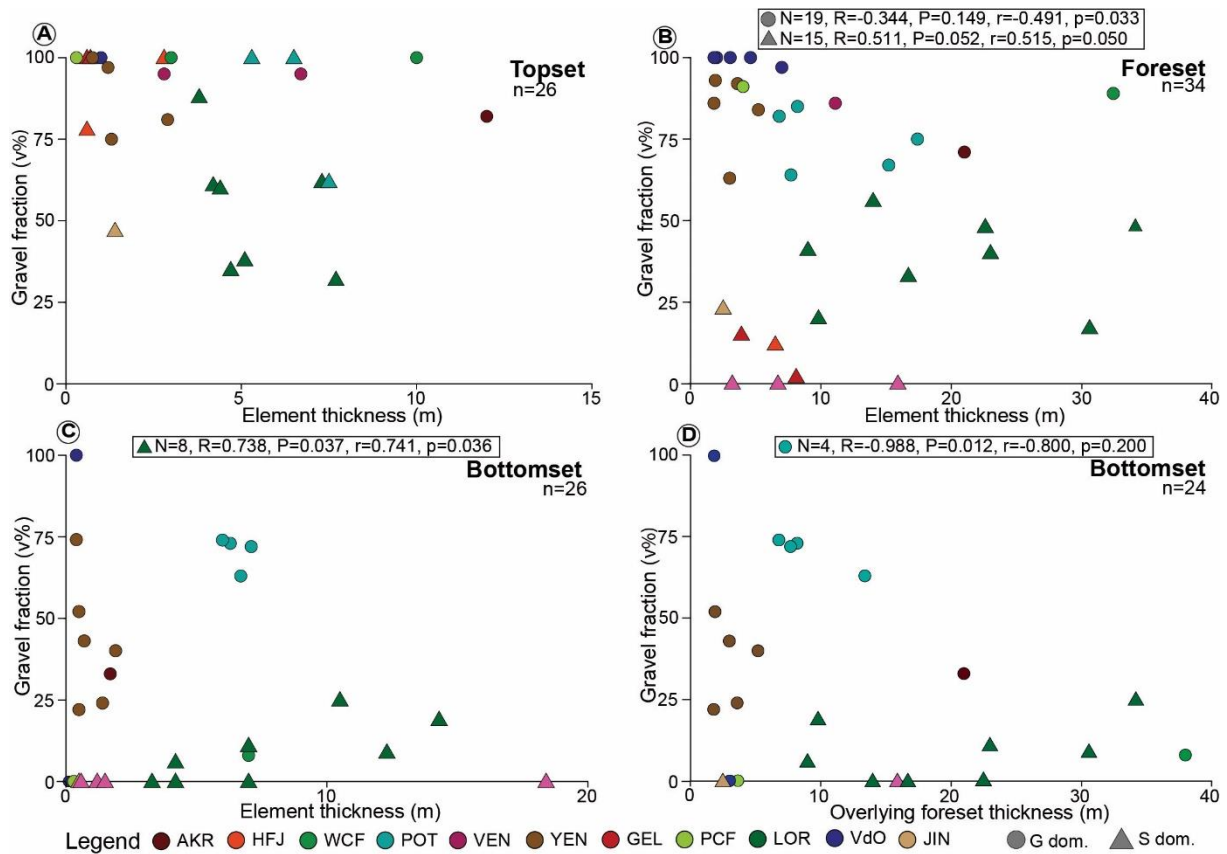
Figure 11 Scatterplots of topset thickness versus gravel fraction (A), foreset thickness versus gravel fraction (B), bottomset thickness versus gravel fraction (C), and foreset thickness versus underlying-bottomset gravel fraction (D). N denotes the size of the dataset, R: Pearsons' R, r: Spearmans' rho. Case study codes can be found in Table 1.

4.3.2.3 Depositional processes

Nine case studies include information about the interpreted depositional processes responsible for the deposition of individual facies units or beds. In the original literature sources, these soft data were mostly summarized as facies codes (e.g., Lee and Chough, 1999) or reported graphically on lithological logs (e.g., Nemec et al., 1999; Ilgar and Nemec, 2005; Gobo et al., 2015). The case studies applied the same nomenclature of interpreted depositional processes (e.g., debris flows, low- to high-density turbidity currents, debris falls), thereby facilitating their comparison.

Based on the proportions of facies categorized by their interpreted depositional processes, it appears that processes vary greatly between gravelly and sandy facies (Fig. 12A). In delta-slope settings, 68% of the total thickness of gravelly facies is linked to debris-flow events, and 26% to turbidity currents. The very small amount of gravel-prone facies (3%) interpreted as associated with low-density turbidity currents in turbidite beds takes the form of thin granule or pebble clusters associated with planar horizontally laminated sands characterized by grain-size fluctuations (Nemec et al., 1999; Gobo et al., 2014a; Leszczyński and Nemec, 2015), or of pebbly basal parts (Gobo et al., 2014b). These granule/pebble clusters are, on average, significantly thinner than gravel beds produced by high-density turbidity currents (mean values: 0.04 m vs. 0.14 m), which themselves are typically thinner than those of debris-flow beds (mean: 0.35 m). Although a minor proportion of the sandy beds was linked to debris flows (8% for sands and 16% for gravelly sands), the majority of sand-prone

deposits were interpreted as laid down by turbidity currents (80-81%). Beds deposited by turbidity currents that underwent hydraulic jump, forming mostly solitary gravelly backsets (Ilgar and Nemec, 2005; Gobo et al., 2014b) (Fig. 12A) on the delta slope, and sand lobes (Nemec et al., 1999) or scour fills at the delta toe (Breda et al., 2009), were reported in several case studies (7 out of 14). However, a significant fraction of sediment formed during hydraulic-jump conditions was only observed at the delta toe, where turbidity currents tend to deposit their coarse load due to flow deceleration and expansion (Ilgar and Nemec, 2005). For example, 18% of the toeset gravel fraction of the Ilias delta (MGCR) was linked to supercritical flows, compared to less than 1% of the overlying delta-slope deposits.

In bottomsets, the percentage of gravel beds interpreted as the products of debris flows or turbidites is approximately the same as that of delta slopes, but the amount of debris-fall sediment decreases (Fig. 12A). Furthermore, debris-flow deposits are represented almost exclusively by gravels. One quarter of the cumulative thickness of gravels linked to turbidity currents were laid down under hydraulic-jump conditions.

The sedimentation on the delta top was largely governed by streamflow processes, locally in combination with subaerial debris flows on fan deltas, and accompanied by wave action and tidal processes in the nearshore. Datasets with quantifiable data on depositional processes were characterized by topsets that are exclusively built by streamflow deposits. The examined delta slopes are dominantly made of the deposits of turbidity currents and debris flows, composing 90% of their cumulative sediment thickness on average (Fig. 13). The third most common depositional process of delta slopes is represented by debris falls, whose deposits rarely reach up to 10% in estimated thickness. The thickness of debris-flow deposits exceeds that of turbidite beds in nearly all deltas (Fig. 13). In foresets, the thickness of turbidite facies relative to that related to both processes varies according to ratios that fall between 1:3 and 1:1 in the majority of cases (Fig. 12B). Bottomsets, however, tend to be dominated by turbiditic deposits, representing 50% to 100% of the cumulative thickness of turbidite and debris-flow sediments (Fig. 12B). Deposits associated with low-density turbidity flows are generally prevalent over those of high-density currents, both on the delta slope and toe. Beds of the latter type are 0.05 m thicker, on average, than their low-density counterparts (0.15 m vs. 0.10 m) and are characterized by less frequent occurrence of planar horizontal lamination (18% vs. 4%). An important difference is seen in the fraction of debris-flow deposits between bottomsets and genetically related overlying foresets, by ca. 40% on average (Fig. 13).

Wave reworking of deltaic deposits is common, especially where beach deposits form a significant part of the topset, but it can also affect the delta slope and toe to varying degrees (Longhitano, 2008). However, a significant cumulative thickness of sediments interpreted as recording wave action is only seen in two of the considered case studies, both being deltas that are less than 9 m thick (Lønne and Nemec, 2004; Ilgar and Nemec, 2005). Although wave action formed gravelly beachfaces in the nearshore, wave reworking affected sandy deposits at greater depths on the delta slope and toe. These processes can alter the estimated thickness of turbidite beds (Fig. 12A). Signatures of tidal processes were also reported from the examined marine examples, but tidal influences appear to have been modest overall (Lønne and Nemec, 2004; Breda et al., 2007; Gobo et al., 2015).
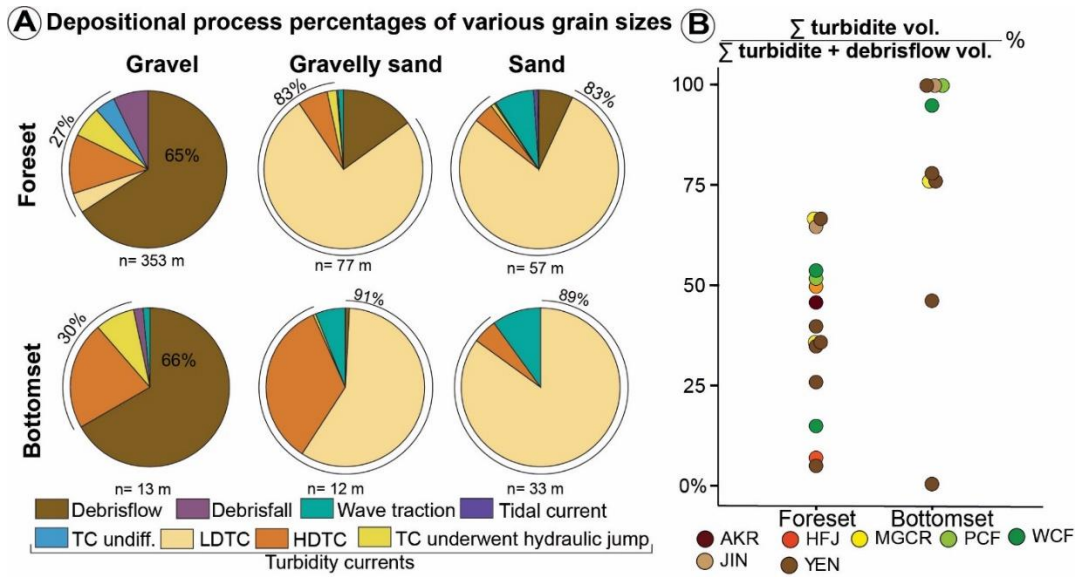
Figure 12 (A) Pie charts showing the proportion of depositional processes interpreted as responsible for the deposition of facies characterized by different grainsizes for foresets and bottomset. (B) Dot plot of the distribution of the calculated turbidite ratio (defined as in formula above the chart) of distinct foresets and bottomsets. Case study codes can be found in Table 1.
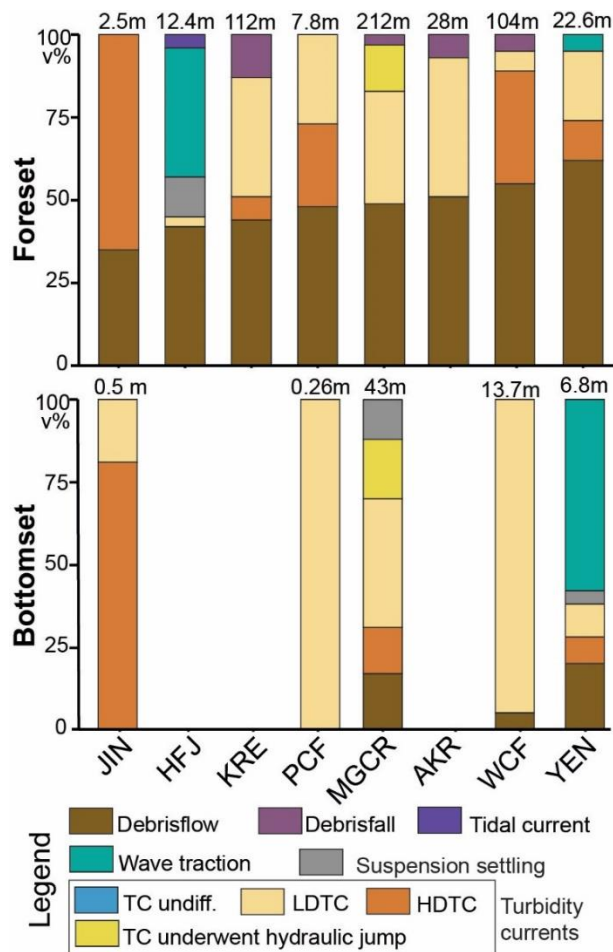

Figure 13 Stacked bar chart showing the proportion of facies linked to specific depositional processes for distinct elements of Gilbert-type deltas of the examined case studies. Numbers above bars represent the total logged thickness of each example. Case study codes can be found in Table 1.

4.3.2.4 Vertical changes in grainsize

An analysis was undertaken to determine vertical changes in the fraction of gravel facies in individual sedimentary logs of delta foresets, and to thereby establish a classification of styles of facies organization of Gilbert-type deltas. Only measured sections that capture the full vertical profile of the delta slope were considered, including cases with missing topset or bottomset (Fig. 6). Sand- and gravel-dominated deltas are represented by 24 and 35 sections, respectively.

The examined foreset units were subdivided into distal, medial and proximal parts, based on a geometric division: each part represents one third of the delta slope measured on the section from top to bottom. The fraction of gravelly facies was calculated for these individual parts and used to classify the vertical profile into coarsening, fining, fining-coarsening, coarsening-fining and uniform (i.e., with no trend) patterns (Fig. 14). In addition, proximal-to-distal trends were characterized in terms of the spatial distribution of gravels through the zones of the delta slope, and an average value of gravel fraction was calculated for each trend (Fig. 14). To investigate how the distribution of gravelly and sandy beds change vertically, proportions of lithologies based on cumulative facies-unit thickness relative to interval thickness were plotted (Fig. 14). Each group of vertical foreset profile type was supplemented by the average grainsize, and data on bed distributions of overlying topsets and underlying bottomsets (Fig. 14).

Most commonly (13 of 34 sections), in gravel-dominated deltas, the distal, medial and proximal foreset parts have approximately (within 10%) the same fraction of gravel facies. The thickness of stacked gravel beds varies over a wide range, with intervals that only rarely are entirely made of gravelly facies (Fig. 14). Thicker coarse beds are usually interbedded with thinner sandy intervals. This type of vertical profile is only seen in deltas with particularly high gravel content (>85% gravel fraction), whereas the other grain-size trends were observed among finer and coarser delta foresets alike (from 50% to 95%). Coarsening-upward foreset sequences are nearly as common (11 of 34); in these, in most cases, the gravel content increases upward in a gradual fashion; in other cases, distal and medial parts exhibit similar gravel fractions. Overall, this grainsize trend is accompanied by an upward increase in the thickness of stacked gravel beds and a concomitant thinning of the sandy units. An opposite trend in bedding properties can be observed in the case of upward-fining delta slopes (5 of 34). Bottomsets underlying upward-fining foresets are coarser on average than those characterized by a different vertical profile (46% vs. 21% respectively). The five foresets characterized by fining-coarsening trends exhibit stacked gravel beds that are thinnest in their medial parts. The thickness of the foresets varies over the same range for all four observed vertical grain-size trends.

For sand-dominated delta slopes, instances where their distal, medial and proximal parts contain near equal amounts of gravel are less common (Fig. 14) and restricted to foresets containing less than 3% gravelly deposits. Coarsening-upward profiles are instead dominant (Fig. 14); in these cases, the distal parts are almost entirely composed of sand, usually, and the thickness of gravelly intervals increases progressively up-section. Coarsening-fining trends were also observed but are less common. They are paralleled by trends of increasing-decreasing thickness of stacked gravel beds. Fining-upward and fining-coarsening trends were not observed. Similarly to gravel-dominated cases, no relationships between foreset thickness and the type of vertical grain-size trend were observed.
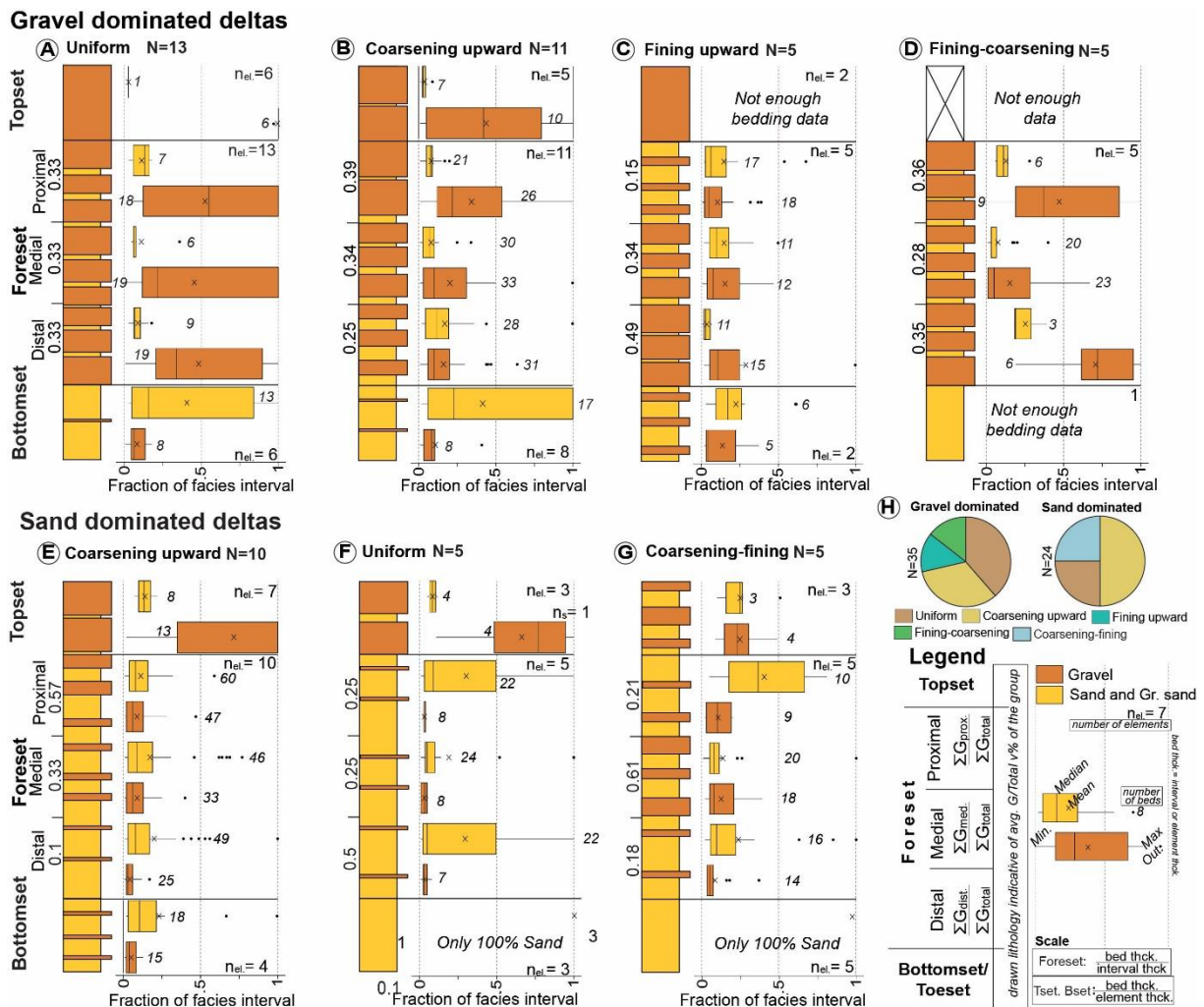
Figure 14 (A-G) Vertical grainsize changes observed in the examined logs of successions of Gibert-type deltas. Bedding trends and average gravel fractions for distal, medial and proximal intervals are also shown. (H) Frequencies of foreset vertical trends for gravel- and sand-dominated deltaic successions.

4.3.2.5 Vertical changes in depositional process

Quantitative data on vertical changes in facies proportions, recording variations in the prevalence of depositional processes, were available for 13 sedimentary logs (Fig. 15), all of which describe delta foresets thinner than 6.5 m. To determine changes in the predominance of turbidites or debris-flow deposits, a 'turbidite ratio' (i.e., the ratio between the cumulative thickness of turbiditic sediments and the total thickness of deposits of turbidites or debris flows; Fig. 12B) was also calculated for the distal, medial and proximal parts of delta slopes, and for bottomsets (Fig. 15). The turbidite ratios of the three distinct delta-slope intervals are characterized by a coefficient of variation of 1.09. On average, the difference between turbidite ratios of successive intervals is 34%, indicating that important variations are seen from proximal to distal parts of delta slopes.

Generally, proximal parts of the delta slope tend to be dominated by debris-flows, with turbidity currents depositing only a quarter of the cumulative thickness of turbidites and debrites. Instead, in distal parts, turbiditic deposits make up 42% of the sediment volume on average. Although the proportion of turbidites can vary markedly, 6 of the 13 examined sections are dominated by products of debris flows along their full profiles

20

(i.e., in distal, medial and proximal intervals; Fig. 15). A decrease in the proportion of turbidites through the delta-slope profile was seen in only four instances. Increasing-decreasing and decreasing-increasing trends in the proportion of turbiditic beds was seen in three sections each.

The examined dataset revealed no observable correlation between the foreset thickness and either the turbidite fraction (N=8, R=-0.114, P=0.789, r=-0.036, p=0.933) or its vertical trends, quantified as the difference in turbidite ratio between the distal and proximal parts of the delta slope in individual sections (N=13, R=-0.135, P=0.661, r=-0.161, p=0.600). Bottomset turbidite ratios also showed no relationship with the overlying foreset thickness (N=6, R=0.071, P=0.893, r=-0.123, p=0.846).

The difference in turbidite ratio between the bottomset and the distal part of the overlying foreset (n=9) is 52% on average. Only three of the nine delta-toe deposits were dominated by debris flows, all from examples in the Yenimahalle Fm. (Table 1). However, the sandy facies of these specific elements were reworked by wave action, which may have overprinted any evidence of their original turbiditic origin.
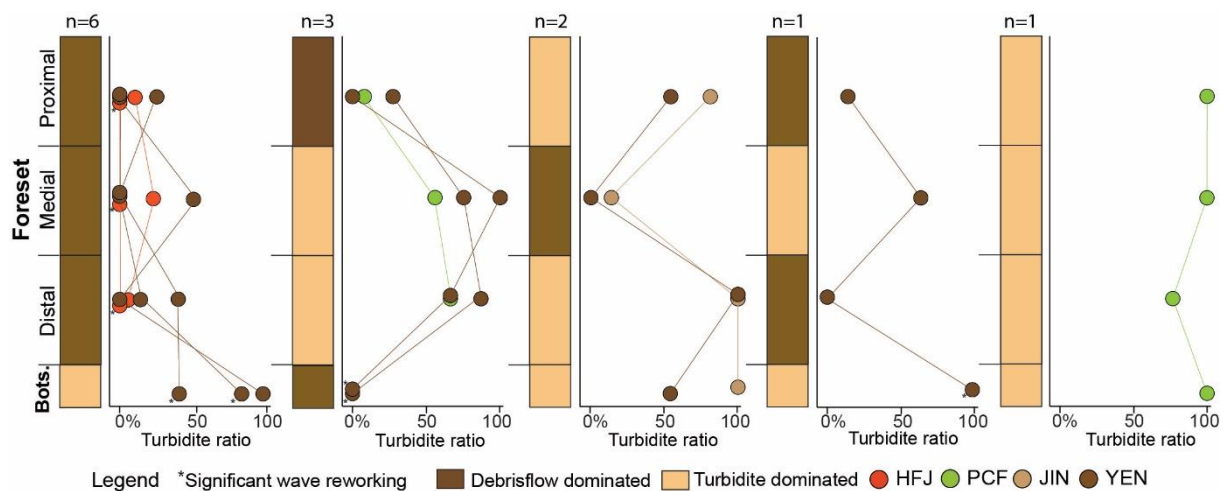

Figure 15 Vertical trends in the relative proportion of sediment of turbidity-flow and debris-flow origin, expressed as turbidite ratio. Case study codes can be found in Table 1.

4.3.3 Basinward changes of delta properties

Gilbert-type deltas can prograde for several kilometres basinward. Therefore, the same delta body might be intersected by multiple boreholes or may be exposed over several outcrops located kilometres apart. Information about the spatial variability in the facies architecture of Gilbert deltas can therefore be used to refine facies models, in a way that they can assist correlations between different sections.

In the dataset, 13 deltaic bodies are included that were described at multiple locations (between two and six sections covering their full vertical profile). For these, it was possible to characterize spatial changes in the different attributes discussed above: element thickness, gravel fraction, dominance of depositional processes, and their expression on vertical profiles (Fig. 16). These data are plotted for the three delta elements, so as to demonstrate how these characteristics change from the point of landward termination of the deltaic edifice to the section that is closer to the basinward delta pinchout (Fig. 16). In all cases, the distance between individual logs was larger than the extent of foreset clinothems, and as such the same clinothem was never

sampled twice. The topsets and bottomsets are not present in every section, due to topset erosion or because bottomsets were not developed at that location.

The architectural elements of the studied deltas vary in size at different locations. Delta slopes are characterized by rapid changes in their thickness close to the point of landward delta nucleation, through progradation over faulted basement or inherited depositional or erosional topography (e.g., LOR, PCF, AKR) (Fig. 1). Over this interval, characterized by abrupt changes in basement geometry, the foreset thickness can increase rapidly, and even double over a horizontal distance of one hundred metres (e.g., LOR: from 6.5 m to 15.2 m foreset growth over 130 m distance, PCF: from 1 m to 2.2 m over 36 m distance). The majority of delta slopes achieved an increase in thickness trough delta progradation, which was accompanied by aggradation and basinward thinning of delta topsets (e.g., AKR, LOR). Delta bottomsets showed no predictable changes in their thickness.

All three types of deltaic architectural elements can show high spatial variability in the fraction of gravelly facies (Fig. 16). The difference between the minimum and maximum proportions of gravel exceeds 15% in 10 out of 15 delta foresets, and in all but one topset and bottomset. This difference is comparable to the variability seen between architectural elements of different deltas of the same or different case studies (Fig. 9). The maximum difference between gravel fractions in the same delta can reach more than 60% for all three elements, and such changes can be abrupt, occurring within a horizontal distance of just 50-75 m (Fig. 16). On average, gravel fraction values measured on individual logs differ from the value calculated for the respective element by 10% for foresets, and by 15% for both topsets and bottomsets. In datasets covering the full dip extent of the deltas, delta foresets can variably show trends of basinward fining, coarsening, or of fairly constant grainsize.

Delta slopes also demonstrate important variability in vertical grainsize trends. The same type of trend is only rarely seen in neighbouring vertical sections of the same unit (only 4 times in 24 adjacent logs), and no systematic basinward change is observed in vertical trends (Fig. 16).

The relative proportion of turbidites and debrites can change significantly in space within the same delta, for both foreset and bottomset elements, which can vary from being debrite dominated to strongly turbidite dominated. On average, adjacent logs through foresets demonstrate a 46% difference in their turbidite ratios; for bottomsets, the average difference is 50%, but this value is based on two deltas only. Similar results were documented by Gobo et al. (2015), when comparing the preserved expression of foreset depositional processes at different locations. Similar spatial variability is seen for the vertical trends in the preserved record of the relative dominance of different depositional processes, with only one of four examined deltas recording the same vertical trend twice (Fig. 16).
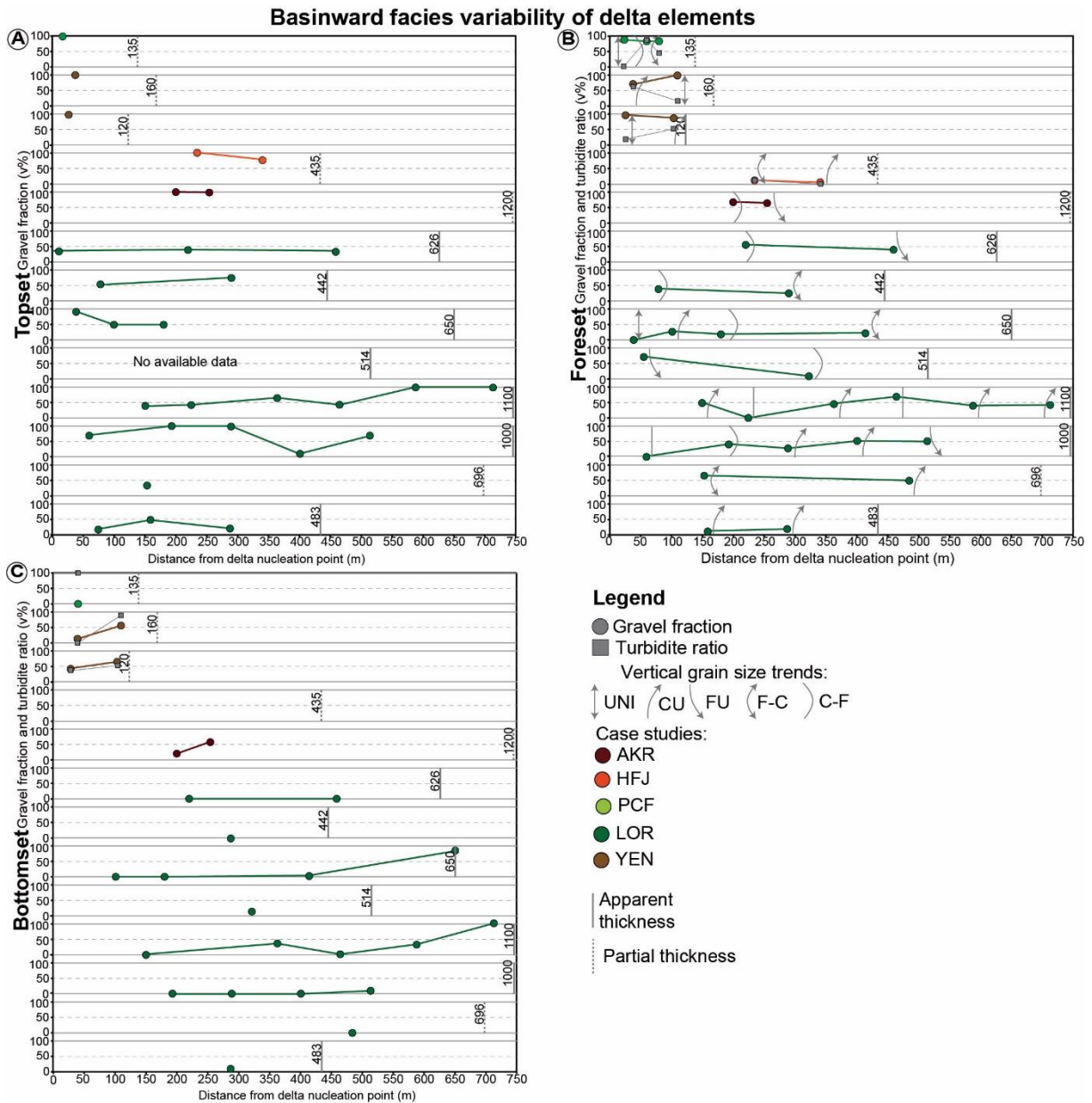
Figure 16 Facies variability of elements of Gilbert-type deltaic bodies: (A) topset, (B) foreset, (C) bottomset; facies characteristics include grainsize, depositional-process predominance and grainsize trends. Case study codes can be found in Table 1.

23

5. Discussion

The studied Gilbert-type deltas show great diversity in their geometry and facies organization, both at the scale of the entire deltaic sedimentary body and of their component architectural elements. The properties of distinct elements are also seen to vary significantly in space, i.e., through the preserved record of the temporal evolution of the deltas.

5.1 Delta dimension

The thickness of Gilbert-type deltas is a direct measure of the sum of (i) the initial depth of the water body into which they built out with continued sediment supply, and (ii) changes in basin depth through deposition, which may be due to relative base-level rise or to delta progradation into deeper basin areas (e.g., Young et al., 2000; Backert et al., 2010; Mortimer et al., 2005). The architectural expression of this is manifested in the observed basinward delta-foreset growth, which is accompanied by an increase in topset thickness when the base level rises in relative terms (Nemec et al., 1999; Uličný et al., 2002; Gobo et al., 2014b; 2015) (Fig. 1).

Analysis of the relationship between thickness and length of 15 deltaic bodies for which accurate data on delta length were available showed positive correlation between the two dimensions. However, deltas with higher (and typically longer) slopes, translating to thicker slope elements, sequester larger sediment volumes along their slopes, and so they may be expected to prograde more slowly: as such, an inverse relationship would instead be expected between delta thickness and length. This could mean that, for the examined examples, thinner deltas may have been characterized by lower rates of sediment supply, which might have resulted in (i) slower progradation rates, and/or (ii) shorter delta lifetimes, in cases where the sediment influx was too limited to contrast base-level rises reversing delta progradation and ultimately leading to delta drowning and abandonment (Postma, 1995; Muto and Steel, 1997). These factors may have limited the ability of the deltas to protrude into deeper depocentres and attain greater lengths and thicknesses. On the contrary, the examined thicker and longer deltas may have been fed by sources delivering sediment at higher rates (e.g., Ilgar and Nemec, 2005; Martini et al., 2017), overcoming the effect of relative base-level rises, and therefore prolonging the lifespan of the deltas, allowing them to reach deeper basin sectors and to form higher (i.e., thicker) slopes (e.g., Young et al., 2000). However, as rates of sediment flux and rate and magnitude of base-level changes are highly dependent on local factors, the observed positive relationship between delta length and thickness is unlikely to be applicable to all Gilbert-type deltas generally. For example, Breda et al. (2009) reported an inverse relationship between delta thickness and length, in relation to how increasing rates of accommodation creation coupled with sediment-supply rates that remain constantly high through the evolution of a delta-hosting incised valley resulted in thinner deltas prograding over longer distances.

Differences in the size of deltas can be due to temporal and spatial variations in the magnitude of accommodation-space generation and in rates of sediment supply even within the same depositional settings, as documented in the examined dataset (Fig. 5), and reported in the case of simultaneously forming deltas (e.g., Martini et al., 2017; Nehyba, 2018; Winsemann et al. 2018). For example, different coeval deltas occurring along the same basin-bounding fault can exhibit physiographic differences in relation to their position, as deltas located closer to the fault tips may receive a larger volume of sediment per unit time, while experiencing lower rates of subsidence, which

collectively can promote their basinward progradation (Gupta et al., 1999; Young et al., 2000). The possible controls of sediment flux on deltaic architectures may be paralleled by variations in facies characteristics that may reflect concomitant changes in sediment calibre; this may be expressed in relationships between delta scale and coarseness, as seen for example in the Loreto Basin deltas (Fig. 5), which were deposited during progressively increasing fault-slip rates, and hence probably under increasing coarse-sediment influx (Mortimer et al., 2005).

5.2 Delta facies

Data on grainsize variability show that the sediment supplied to Gilbert-type deltas can vary widely with regards to gravel content, and that sand- and gravel-dominated deltas are characterized by contrasting facies arrangements. Although sand-dominated deltas are characterized by sandy foreset and bottomset elements, their topsets, similarly to those of gravel-dominated systems, are dominated by gravels (Fig. 8). This indicates that a coarse fluvial feeder system and significant subaerial sand bypass are common across all the studied Gilbert-type deltas. In gravel-dominated deltas, the delta slopes tend to coarsen in parallel with the increase in gravel content in the feeder fluvial distributary system (Fig. 9A), while foresets tend to be finer when they are thicker (Fig. 11B). The latter can be explained by how, along higher slopes, debris flows, carrying higher amount of coarse material than turbidity currents, tend to either undergo frictional freezing in the medial and proximal sectors, thereby having shorter runout distances, or evolve into turbidity currents after disentrainment of the bulk of their coarse load. Due to the greater length of the delta slope, these linked turbidity currents, along with the ones generated at the river mouth, can deposit at least part of their finer load on the foreset; in contrast, on shorter slopes, the majority of the sandy material can bypass the foreset and be deposited at the bottomset (Nemec, 1990, 1999; Sohn et al., 1997; Falk and Dorsey, 1998; Breda et al., 2007; McConnico and Bassett, 2007). Possible evidence of this is in the negative correlation between bottomset gravel fraction and overlying foreset thickness seen in the examples from the Potenza Basin (Longhitano, 2008).

5.3 Basinward facies changes

Examination of different logged sections through individual deltas showed great spatial variability in internal facies characteristics, with delta elements showing gravel fractions that differ by up to 15% at different locations compared to their average. Despite this spatial variability, the gravel fraction of the foresets of both gravel and sand-dominated deltas measured in individual logs rarely falls below or exceeds 50% (Fig. 16B). These changes in grain size are also coupled with variations in turbidite ratios and with different vertical trends in grain size and depositional processes in neighbouring sections. This variability in facies organization can be related to both autogenic mechanisms and allogenic factors, such as influences by climate (even at seasonal scale) and tectonics on sediment calibre and rate of supply (Postma, 1995, 2001; Dorsey, 1997; Kleinhans, 2005; Longhitano, 2008; Breda et al., 2009; Corner, 2011; Eilertsen et al., 2011; Gobo et al., 2014b; Winsemann et al., 2018, 2021). Grainsize fluctuations can be induced or enhanced autogenically, notably by river avulsions, leading to lobe switching and to changes in the directions of sediment dispersal to the delta front and slope (Dorsey, 1997; Kleinhans, 2005; Longhitano, 2008). Another form of autogenic control is exerted by the growth of the alluvial distributary system through the evolution of a delta: deltaic progradation drives the sequestration of coarse material on the topsets, causing a progressive reduction in coarse sediment input to the

subaqueous delta (Prior and Bornhold, 1990; Breda et al., 2009). Notably, however, no basinward trends in the grainsize of topset deposits were observed in this study; yet, the considered datasets had limited three-dimensional control, and likely only sampled a small portion of delta-top elements that were presumably architecturally complex.

The spatial changes documented in the relative dominance of foreset and bottomset sedimentary processes, and the important differences in turbidite ratio between the medial, distal and proximal portions of the delta slope (Fig. 15) can indicate intermittent temporal changes in the predominance of debris flows or turbidity currents during delta evolution. These changes can also be induced by climatic or tectonic allogenic factors influencing sediment dispersal to the delta front, for example through the effect of short-term base-level fluctuations through delta progradation (Gobo et al., 2015). During periods of base-level rise, local accommodation space is generated at the delta front, leading to increased sediment storage and frequent gravitational collapses that can result in a debrite-dominated foreset assemblage. Base-level stillstands may instead be characterized by the dominance of turbidity currents where hyperpycnal river effluents feed sediment to the delta slope (Gobo et al., 2015; Winsemann et al., 2018). Base-level drops, instead, can promote the formation of debris flows and chute-fill deposits due to delta erosion (Ilgar and Nemec, 2005; Winsemann et al., 2018; Kostic et al., 2019). As no relationship was observed between the delta slope height (i.e., thickness) and neither the turbidite ratio nor its vertical changes, it can be inferred that base-level fluctuations may have exerted a stronger control on temporal changes in the prevalence of turbidity flows on the delta slope (manifested in vertical profiles), compared to flow transformation, which is instead expected to result in an increase in the proportion of turbiditic deposits towards the delta toe (Sohn et al., 1997; Falk and Dorsey, 1998; Nemec et al., 1999). However, it is worth noting that a bias exists, whereby the studied deltas for which the relative dominance of sedimentary processes could be quantified for the whole length of the delta slope all exhibit thin foresets (<6.5 m); the limited bathymetry of their delta toes might have allowed debris flows to run out relatively more distally. Notwithstanding, Gobo et al. (2014b) showed that debris flows originating from chute-wall collapse can reach the toeset and bottomset even for high delta slopes, during periods when delta-slope deposition is dominated by turbidity currents.

5.4 Applications

The findings of this study can be applied to place outcrop observations in the context of a general facies model for Gilbert-type deltas, and to help assess the suitability of certain successions as geological analogues for subsurface studies, quantitatively.

The documented variability of vertical grain-size trends, element proportions and dimensions can be used to aid the recognition of Gilbert-type deltas in boreholes where their diagnostic tripartite internal architecture and the presence of steeply dipping foresets are not observable. The relationships between thickness and length of the examined deltas can instead aid the prediction of the lateral extent of such deltas whenever their vertical extent has been observed or inferred.

The highlighted internal facies variability of the studied deltas indicates that different borehole sections of deltaic bodies characterized by contrasting vertical profiles, gravel fraction and turbidite ratio do not necessarily intersect different deltas; this should be taken into consideration for physical stratigraphic correlation across different borehole

sections, along with information on the likely lateral extent of a deltaic body. Furthermore, the presented characterization of lateral and vertical changes in facies make-up can be referred to when attempting predictions of the spatial variability in sedimentary heterogeneity of subsurface successions.

6 Conclusions

A database-driven analysis of 62 deltaic successions was undertaken to characterize and quantify the architectural and facies variability of Gilbert-type deltas. Some key findings can be summarised as follows:

- The thickness of the studied Gilbert-type deltas ranges between 2 m to over 650 m and their lengths from hundreds to thousands of metres. The interplay between changes in sediment supply and base level may explain the positive relationship between delta thickness and length. However, as the importance of these factors vary widely within and across basins, this observation cannot be applied universally in a predictive way.
- Gilbert-type deltas vary from dominantly sandy to almost exclusively gravelly. Both sandy and gravelly types show a fining trend from the delta top to the delta toe, and both are usually characterized by gravel-prone topsets. Gravel-dominated examples show a positive relationship between topset and foreset gravel fractions, and foresets tend to be finer when they are thicker.
- The studied Gilbert-type deltas showed important spatial variability in grain size and interpreted depositional process, and in their vertical trends. These variations within individual deltaic bodies can be linked to changes in base level and sediment influx resulting from controls exerted by climate and tectonics, or from autogenic dynamics of the fluvial feeder system (e.g., channel avulsion) during delta evolution.
- Outcomes of the analysis carried out in this study can aid: (i) the recognition of Gilbert-type deltaic bodies in boreholes, (ii) the prediction of the vertical and basinward extent and sedimentary heterogeneity of the identified deltas, and (iii) the correlation of deltaic bodies across multiple boreholes or outcrops. Moreover, this study provides a general template of the quantifiable properties of Gilbert-type deltas and describes the inherent variability of geological analogues that may be considered for subsurface interpretations and predictions.

References

Backert, N., Ford, M., Malartre, F., 2010. Architecture and sedimentology of the Kerinitis Gilbert-type fan delta, Corinth Rift, Greece. Sedimentology 57, 543–586. https://doi.org/10.1111/j.1365-3091.2009.01105.x

Barrell, J., 1912. Criteria for the recognition of ancient delta deposits. Geological Society of America Bulletin 23, 377–446. https://doi.org/10.1130/GSAB-23-377

Bestland, E.A., 1991. A Miocene Gilbert-type fan-delta from a volcanically influenced lacustrine basin, Rusiga Island, Lake Victoria, Kenya. Journal of the Geological Society, London 148, 1067–1078. https://doi.org/10.1144/gsjgs.148.6.1067

Bowman, D., 1990. Climatically triggered Gilbert-type lacustrine fan deltas, the Dead Sea area, Israel. In: Colella, A., Prior, B.D. (Eds.), Coarse-Grained Deltas. International Association of Sedimentologists Special Publication, vol. 10, Blackwell Scientific Publications, pp. 273–280. https://doi.org/10.1002/9781444303858.ch15

Breda, A., Mellere, D., Massari, F., 2007. Facies and processes in a Gilbert-delta-filled incised valley (Pliocene of Ventimiglia, NW Italy). Sedimentary Geology 200, 31–55. https://doi.org/10.1016/j.sedgeo.2007.02.008

Breda, A., Mellere, D., Massari, F., Asioli, A., 2009. Vertically stacked Gilbert-type deltas of Ventimiglia (NW Italy): The Pliocene record of an overfilled Messinian incised valley. Sedimentary Geology 219, 58–76. https://doi.org/10.1016/j.sedgeo.2009.04.010

Chough, S.K., Hwang, I.G., 1997. The Duksung Fan Delta, Se Korea: Growth of Delta Lobes on a Gilbert-Type Topset in Response to Relative Sea-Level Rise. Journal of Sedimentary Research 67, 725-739. https://doi.org/10.1306/d4268626-2b26-11d7-8648000102c1865d

Chough, S.K., Hwang, I.G., Choe, M.Y., 1990. The Miocene Doumsan Fan-Delta, Southeast Korea: A Composite Fan-Delta System in Back-Arc Margin. Journal of Sedimentary Research 60, 445–455. https://doi.org/10.1306/212F91BA-2B24-11D7-8648000102C1865D

Ciampalini, A., Firpo, M., 2015. Depositional architecture and sequence stratigraphy of pleistocene coarse-grained deltas along the Ligurian coast (Italy). Journal of Earth System Science 124, 1765–1780. https://doi.org/10.1007/s12040-015-0640-3

Colella, A., 1988. Fault-controlled marine Gilbert-type fan deltas. Geology 16, 1031–1034. https://doi.org/10.1130/0091-7613(1988)016<1031:FCMGTF>2.3.CO;2

Colella, A., De Boer, P.L., Nio, S.D., 1987. Sedimentology of a marine intermontane Pleistocene Gilbert-type fan-delta complex in the Crati Basin, Calabria, southern Italy. Sedimentology 34, 721–736. https://doi.org/10.1111/j.1365-3091.1987.tb00798.x

Colombera, L., Mountney, N.P., Hodgson, D.M., McCaffrey, W.D., 2016. The Shallow-Marine Architecture Knowledge Store: A database for the characterization of shallow-marine and paralic depositional systems. Marine and Petroleum Geology 75, 83–99. https://doi.org/10.1016/j.marpetgeo.2016.03.027

Corner, G.D., 2011. A Transgressive-Regressive Model of Fjord-Valley Fill:

Stratigraphy, Facies and Depositional Controls. In: Dalrymple, R.W., Leckie D.A., Tillman, R.W. (Eds.) Incised Valleys in Time and Space. SEPM Special Publication 85, pp. 161–178. https://doi.org/10.2110/pec.06.85.0161

Dart, C.J., Collier, R.E.L., Gawthorpe, R.L., Keller, J.V.A., Nichols, G., 1994. Sequence stratigraphy of (?)Pliocene-Quaternary synrift, Gilbert-type fan deltas, northern Peloponnesos, Greece. Marine and Petroleum Geology 11, 545-560. https://doi.org/10.1016/0264-8172(94)90067-1

Dorsey, R.J., 1997. Earthquake clustering inferred from Pliocene Gilbert-type fan deltas in the Loreto basin, Baja California Sur, Mexico. Geology 25, 679–682. https://doi.org/10.1130/0091-7613(1997)025<0679:ECIFPG>2.3.CO;2

Dorsey, R.J., Umhoefer, P.J., Renne, P.R., 1995. Rapid subsidence and stacked Gilbert-type fan deltas, Pliocene Loreto basin, Baja California Sur, Mexico. Sedimentary Geology 98, 181–204. https://doi.org/10.1016/0037-0738(95)00032-4

Dunne, L.A., Hempton M.R., 1984. Deltaic sedimentation in the Lake Hazar pull-apart basin, south-eastern Turkey. Sedimentology 31, 401-412. https://doi.org/10.1111/j.1365-3091.1984.tb00868.x

Eilertsen, R.S., Corner, G.D., Aasheim, O., Hansen, L., 2011. Facies characteristics and architecture related to palaeodepth of Holocene fjord-delta sediments. Sedimentology 58, 1784–1809. https://doi.org/10.1111/j.1365-3091.2011.01239.x

Falk, P.D., Dorsey, R.J., 1998. Rapid development of gravelly high-density turbidity currents in marine Gilbert-type fan deltas, Loreto Basin, Baja California Sur, Mexico. Sedimentology 46, 331–349. https://doi.org/10.1046/j.1365-3091.1998.0153e.x

Ferentinos, G., Papatheodorou, G., Collins, M.B., 1988. Sediment Transport processes on an active submarine fault escarpment: Gulf of Corinth, Greece. Marine Geology 83, 43–61. https://doi.org/10.1016/0025-3227(88)90051-5

García-García, F., Fernández, J., Viseras, C., Soria, J.M., 2006a. High frequency cyclicity in a vertical alternation of Gilbert-type deltas and carbonate bioconstructions in the late Tortonian, Tabernas Basin, Southern Spain. Sedimentary Geology 185, 79-92. https://doi.org/10.1016/j.sedgeo.2006.03.025

García-García, F., Fernández, J., Viseras, C., Soria, J.M., 2006b. High frequency cyclicity in a vertical alternation of Gilbert-type deltas and carbonate bioconstructions in the late Tortonian, Tabernas Basin, Southern Spain. Sedimentary Geology 192, 123-139. https://doi.org/10.1016/j.sedgeo.2006.03.025

Gawthorpe R.L., Colella. A., 1990. Tectonic Controls on Coarse-Grained Delta Depositional Systems in Rift Basins, In: Colella, A., Prior, D.B. (Eds.), Coarse-Grained Deltas. International Association of Sedimentologists Special Publication, vol. 10, Blackwell Scientific Publications, pp. 113–127. https://doi.org/10.1002/9781444303858.ch6

Geehan, G., Underwood, J., 1993. The Use of Length Distributions in Geological Modelling, In: Flint, S.S., Bryant, I.D. (Eds.), The Geological Modelling of Hydrocarbon Reservoirs and Outcrop Analogues, IAS Special Publication, 15. pp.

205–212. https://doi.org/10.1002/9781444303957.ch13

Ghinassi, M., 2007. The effects of differential subsidence and coastal topography on high-order transgressive-regressive cycles: Pliocene nearshore deposits of the Val d'Orcia Basin, Northern Apennines, Italy. Sedimentary Geology 202, 677–701. https://doi.org/10.1016/j.sedgeo.2007.08.002

Gilbert, G.K., 1885. The topographic features of lake shores. U.S. Geological Survey Annual Report 5, 69–123.

Gobo, K., Ghinassi, M., Nemec, W., Sjursen, E., 2014a. Development of an incised valley-fill at an evolving rift margin : Pleistocene eustasy and tectonics on the southern side of the Gulf of Corinth, Greece. Sedimentology 61, 1086–1119. https://doi.org/10.1111/sed.12089

Gobo, Ghinassi, M., Nemec, W., 2014b. Reciprocal Changes In Foreset To Bottomset Facies In A Gilbert-Type Delta: Response To Short-Term Changes In Base Level. Journal of Sedimentary Research 84, 1079–1095. https://doi.org/10.2110/jsr.2014.83

Gobo, K., Ghinassi, M., Nemec, W., 2015. Gilbert-type deltas recording short-term base-level changes: Delta-brink morphodynamics and related foreset facies. Sedimentology 62, 1923–1949. https://doi.org/10.1111/sed.12212

Gupta, S., Underhill, J.R., Sharp, I.R., Gawthorpe, R.L., Ract, A., 1999. Role of fault interactions in controlling synrift sediment dispersal patterns: Miocene, Abu Alaqa Group, Suez Rift, Sinai, Egypt. Basin Research 11, 167–189. https://doi.org/10.1046/j.1365-2117.1999.00300.x

Gutsell, J.E., Clague, J.J., Best, M.E., Bobrowsky, P.T., Hutchinson, I., 2004. Architecture and evolution of a fjord-head delta, western Vancouver Island, British Columbia. Journal of Quaternary Science 19, 497–511. https://doi.org/10.1002/jqs.844

Hwang, I.G., Chough, S.K., 2000. The Maesan fan delta, Miocene Pohang Basin, SE Korea: Architecture and depositional processes of a high-gradient fan-delta-fed slope system. Sedimentology 47, 995–1010. https://doi.org/10.1046/j.1365-3091.2000.00335.x

Ilgar, A., 2015. Miocene sea-level changes in northernmost Anatolia: Sedimentary record of eustasy and tectonism at the peri-Pontide fringe of Eastern Paratethys. Sedimentary Geology 316, 62–79. https://doi.org/10.1016/j.sedgeo.2014.11.006

Ilgar, A., Nemec, W., 2005. Early Miocene lacustrine deposits and sequence stratigraphy of the Ermenek Basin, Central Taurides, Turkey. Sedimentary Geology 173, 233–275. https://doi.org/10.1016/j.sedgeo.2003.07.007

Kleinhans, M.G., 2005. Autogenic cyclicity of foreset sorting in experimental Gilbert-type deltas. Sedimentary Geology 181, 215-224. https://doi.org/10.1016/j.sedgeo.2005.09.001

Kostic, B., Becht, A., Aigner, T., 2005. 3-D sedimentary architecture of a Quaternary gravel delta (SW-Germany): Implications for hydrostratigraphy. Sedimentary Geology 181, 147–171. https://doi.org/10.1016/j.sedgeo.2005.07.004

Kostic, S., Casalbore, D., Chiocci, F., Lang, J., Winsemann, J., 2019. Role of upper-

flow-regime bedforms emplaced by sediment gravity flows in the evolution of deltas. Journal of Marine Science and Engineering 7, 5. https://doi.org/10.3390/jmse7010005

Lang, J., Winsemann J., 2013. Lateral and vertical facies relationships of bedforms deposited by aggrading supercritical flows: From cyclic steps to humpback dunes. Sedimentary Geology 296, 36-54. http://dx.doi.org/10.1016/j.sedgeo.2013.08.005

Lang, J., Siever, J., Loewer, M., Igel. J., Winsemann, J., 2017. 3D architecture of cyclic-step and antidune deposits in glacigenic subaqueous fan and delta settings: Integrating outcrop and ground-penetrating radar data. Sedimentary Geology 362, 83-100. https://doi.org/10.1016/j.sedgeo.2017.10.011

Lang, J., Le Heron, D.P., Van den Berg, J.H., Winsemann, J., 2021. Bedforms and sedimentary structures related to supercritical flows in glacigenic settings. Sedimentology 68, 1539-1579. 10.1111/sed.12776

Lee, S.H., Chough, S.K., 1999. Progressive changes in sedimentary facies and stratal patterns along the strike-slip margin, northeastern Jinan Basin (Cretaceous), southwest Korea: Implications for differential subsidence. Sedimentary Geology 123, 81–102. https://doi.org/10.1016/S0037-0738(98)00087-6

Leren, B.L.S., Howell, J., Enge, H., Martinius, A.W., 2010. Controls on stratigraphic architecture in contemporaneous delta systems from the Eocene Roda Sandstone, Tremp-Graus Basin, northern Spain. Sedimentary Geology 229, 9–40. https://doi.org/10.1016/j.sedgeo.2010.03.013

Leszczyński, S., Nemec, W., 2015. Dynamic stratigraphy of composite peripheral unconformity in a foredeep basin. Sedimentology 62, 645–680. https://doi.org/10.1111/sed.12155

Longhitano, S.G., 2008. Sedimentary facies and sequence stratigraphy of coarse-grained Gilbert-type deltas within the Pliocene thrust-top Potenza Basin (Southern Apennines, Italy). Sedimentary Geology 210, 87–110. https://doi.org/10.1016/j.sedgeo.2008.07.004

Lønne, I., Nemec, W., 2004. High-arctic fan delta recording deglaciation and environment disequilibrium. Sedimentology 51, 553–589. https://doi.org/10.1111/j.1365-3091.2004.00636.x

Lowe, D.R., 1982. Sediment Gravity Flows : II. Depositional models with special reference to the deposits of high-density turbidity currents. Journal of Sedimentary Petrology 52, 279–297. https://doi.org/10.1306/212F7F31-2B24-11D7-8648000102C1865D

Martini, I., Ambrosetti, E., Sandrelli, F., 2017. The role of sediment supply in large-scale stratigraphic architecture of ancient Gilbert-type deltas (Pliocene Siena-Radicofani Basin, Italy). Sedimentary Geology 350, 23–41. https://doi.org/10.1016/j.sedgeo.2017.01.006

Massari, F., 1996. Upper-Flow-Regime Stratification Types on Steep-Face, Coarse-Grained, Gilbert-Type Progradational Wedges (Pleistocene, Southern Italy). Journal of Sedimentary Research 66, 364-375. https://doi.org/10.1306/D426834C-2B26-11D7-8648000102C1865D

Massari, F., 2017. Supercritical-flow structures (backset-bedded sets and sediment waves) on high-gradient clinoform systems influenced by shallow-marine hydrodynamics. Sedimentary Geology 360, 73-95. https://doi.org/10.1016/j.sedgeo.2017.09.003

Massari, F., Parea, G.C., 1990. Wave-dominated Gilbert-type gravel deltas in the hinterland of the Gulf of Taranto (Pleistocene, southern Italy). In: Colella, A., Prior, D.B. (Eds.), Coarse-Grained Deltas. International Association of Sedimentologists Special Publication, vol. 10, Blackwell Scientific Publications, pp. 311–331. https://doi.org/10.1002/9781444303858.ch18

McConnico, T.S., Bassett, K.N., 2007. Gravelly Gilbert-type fan delta on the Conway Coast, New Zealand: Foreset depositional processes and clast imbrications. Sedimentary Geology 198, 147–166. https://doi.org/10.1016/j.sedgeo.2006.05.026

Mortimer, E., 2004. Tectonic controls on the growth of coarse-grained delta clinoforms in the Pliocene Loreto Basin, Baja California Sur, Mexico (Ph.D. Thesis). University of Edinburgh, Edinburgh, Scotland.

Mortimer, E., Gupta, S., Cowie, P., 2005. Clinoform nucleation and growth in coarse-grained deltas, Loreto basin, Baja California Sur, Mexico: A response to episodic accelerations in fault displacement. Basin Research 17, 337–359. https://doi.org/10.1111/j.1365-2117.2005.00273.x

Muto, T., Steel, R.J., 1997. Principles of regression and transgression: The nature of the interplay between accommodation and sediment supply. Journal of Sedimentary Research 67, 994–1000. https://doi.org/10.1306/d42686a8-2b26-11d7-8648000102c1865d

Nehyba, S., 2018. Lower Badenian coarse-grained Gilbert deltas in the southern margin of the Western Carpathian Foredeep basin. Geologica Carpathica 69, 89–113. https://doi.org/10.1515/geoca-2018-0006

Nemec, W., 1990. Aspects of Sediment Movement on Steep Delta Slopes, In: Colella, A., Prior, D.B. (Eds.), Coarse-Grained Deltas. International Association of Sedimentologists Special Publication, vol. 10, Blackwell Scientific Publications, pp. 29–73. https://doi.org/10.1002/9781444303858.ch3

Nemec, W., 1995. The dynamics of deltaic suspension plumes, In: Oti, M.N., Postma, G. (Eds.), Geology of Deltas. AA Balkema, Rotterdam, pp. 31–93.

Nemec, W., Lønne, I., Blikra, L.H., 1999. The Kregnes moraine in Gauldalen, west-central Norway: Anatomy of a Younger Dryas proglacial delta in a palaeofjord basin. Boreas 28, 454–476. https://doi.org/10.1111/j.1502-3885.1999.tb00234.x

Nemec, W., Steel, R.J., 1988. What is fan delta and how do we recognize it? In: Nemec W., Steel R.J. (Eds.) Fan Deltas: Sedimentology and Tectonic Settings. Blackie and Son, London, pp. 3–13.

Németh, K., Martin, U., Harangi, S., 2001. Miocene phreatomagmatic volcanism at Tihany (Pannonian Basin, Hungary). Journal of Volcanology and Geothermal Research 111, 111–135. https://doi.org/10.1016/S0377-0273(01)00223-2

Postma, G., 1984. Slumps and their deposits in fan delta front and slope. Geology 12, 27–30. https://doi.org/10.1130/0091-7613(1984)12<27:SATDIF>2.0.CO;2

Postma, G., 1990. Depositional architecture and facies of river and fan deltas: a synthesis, In: Colella, A., Prior, B.D. (Eds.), Coarse-Grained Deltas. International Association of Sedimentologists Special Publication, vol. 10, Blackwell Scientific Publications, pp. 13–27. https://doi.org/10.1002/9781444303858.ch2

Postma, G., 1995. Sea-level-related architectural trends in coarse-grained delta complexes. Sedimentary Geology 98, 3–12. https://doi.org/10.1016/0037-0738(95)00024-3

Postma, G., 2001. Physical climate signatures in shallow- and deep-water deltas. Global and Planetary Change 28, 93–106. https://doi.org/10.1016/S0921-8181(00)00067-9

Postma, G., Roep, T., 1985. Resedimented Conglomerates in the Bottomsets of Gilbert-type Gravel Deltas. Journal of Sedimentary Petrology 55, 874–885. https://doi.org/10.1306/212f882d-2b24-11d7-8648000102c1865d

Postma, G., Lang, J., Hoyal, D.C., Fedele, J.J., Demko, T., Abreu, V., Pederson, K.H., 2021. Reconstruction of bedform dynamics controlled by supercritical flow in the channel–lobe transition zone of a deep-water delta (Sant Llorenç del Munt, northeast Spain, Eocene). Sedimentology 68, 1674-1697. 10.1111/sed.12735

Prior, B.D., Bornhold, B.D., 1990. The underwater development of Holocene fan deltas, In: Colella, A., Prior, B.D. (Eds.), Coarse-Grained Deltas. International Association of Sedimentologists Special Publication, vol. 10, Blackwell Scientific Publications, pp. 75–90. https://doi.org/10.1002/9781444303858.ch4

Rees, C., Palmer, J., Palmer, A., 2018. Gilbert-style Pleistocene fan delta reveals tectonic development of North Island axial ranges, New Zealand. New Zealand Journal of Geology and Geophysics 61, 64–78. https://doi.org/10.1080/00288306.2017.1406377

Rohais, S., Eschard, R., Guillocheau, F., 2008. Depositional model and stratigraphic architecture of rift climax Gilbert-type fan deltas (Gulf of Corinth, Greece). Sedimentary Geology 210, 132–145. https://doi.org/10.1016/j.sedgeo.2008.08.001

Rubi, R., Rohais, S., Bourquin, S., Moretti, I., Desaubliaux, G., 2018. Processes and typology in Gilbert-type delta bottomset deposits based on outcrop examples in the Corinth Rift. Marine and Petroleum Geology 92, 193–212. https://doi.org/10.1016/j.marpetgeo.2018.02.014

Schneider, C.A., 2012. NIH Image to ImageJ: 25 years of image analysis. Nature Methods 9, 671-675. https://doi.org/10.1038/nmeth.2089

Smith, D.G., Jol, H.M., 1997. Radar structure of a Gilbert-type delta, Peyto Lake, Banff National Park, Canada. Sedimentary Geology 113, 195–209. https://doi.org/10.1016/S0037-0738(97)00061-4

Sohn, Y.K., Kim, S.B., Hwang, I.G., Bahk, J.J., Choe, M.Y., Chough, S.K., 1997. Characteristics and depositional processes of large-scale gravelly Gilbert-type foresets in the Miocene Doumsan fan delta, Pohang Basin, SE Korea. Journal of Sedimentary Research 67, 130-141. https://doi.org/10.1306/D4268513-2B26-11D7-8648000102C1865D

Soria, J.M., Fernández, J., García, F., Viseras, César, 2003. Correlative lowstand deltaic and shelf systems in the Guadix Basin (Late Miocene, Betic Cordillera, Spain): The stratigraphic record of forced and normal regressions. Journal of Sedimentary Research 73, 912–925. https://doi.org/10.1306/031103730912

Sztanó, O., Magyari, Á., Tóth, P., 2010. Gilbert-type delta in the Pannonian Kálla Gravel near Tapolca, Hungary. Földtani Közlöny 140, 167–182.

Uličný, D., Nichols, G., Waltham, D., 2002. Role of initial depth at basin margins in sequence architecture: Field examples and computer models. Basin Research 14, 347–360. https://doi.org/10.1046/j.1365-2117.2002.00183.x

Winsemann, J., Lang, J., Polom, U., Loewer, M., Igel, J., Pollok, L., Brandes, C., 2018. Ice-marginal forced regressive deltas in glacial lake basins: geomorphology, facies variability and large-scale depositional architecture. Boreas 47, 973–1002. https://doi.org/10.1111/bor.12317

Winsemann, J., Lang, J., Fedele., J., Hoyal D.C.J.D., 2021. Re-examining models of shallow-water deltas: Insights from tank experiments and field examples. Sedimentary Geology 421, 105962. https://doi.org/10.1016/j.sedgeo.2021.105962

Young, M.J., Gawthorpe, R.L., Sharp, I.R., 2000. Sedimentology and sequence stratigraphy of a transfer zone coarse-grained delta, Miocene Suez Rift, Egypt. Sedimentology 47, 1081–1104. https://doi.org/10.1046/j.1365-3091.2000.00342.x

Zelilidis, A., Kontopoulos, N., 1996. Significance of fan deltas without toe-sets within rift and piggy-back basins: Examples from the corinth graben and the mesohellenic trough, Central Greece. Sedimentology 43, 253–262. https://doi.org/10.1046/j.1365-3091.1996.d01-3.x